引用格式：王东明，胡健民，赵远方，等，2026. 华北克拉通新太古代晚期鲁西造山带的物质组成、构造格架及构造演化过程[J]. 地质力学学报，32（2）：285−311. DOI：10.12090/j.issn.1006-6616.2025033

Citation: WANG D M，HU J M，ZHAO Y F，et al.，2026. Composition, tectonic framework, and evolution of the Luxi Orogenic Belt in the North China Craton during the Late Neoarchean[J]. Journal of Geomechanics，32（2）：285−311. DOI：10.12090/j.issn.1006-6616.2025033

华北克拉通新太古代晚期鲁西造山带的物质组成、构造格架及构造演化过程

王东明[1]，胡健民[2]，赵远方[2]，闫纪元[3]，公王斌[2]，张志刚[4]

WANG Dongming[1]，HU Jianmin[2]，ZHAO Yuanfang[2]，YAN Jiyuan[3]，GONG Wangbin[2]，ZHANG Zhigang[4]

1. 龙岩学院，福建 龙岩 364012；
2. 中国地质科学院地质力学研究所，北京 100081；
3. 中国地震应急搜救中心，北京 100049；
4. 山东省地质调查院，山东 济南 250013

1. *Longyan University*, *Longyan* 364012, *Fujian*, *China*;
2. *Institute of Geomechanics*, *Chinese Academy of Geological Sciences*, *Beijing* 100081, *China*;
3. *National Earthquake Response Support Service*, *Beijing* 100049, *China*;
4. *Shandong Institute of Geological Survey*, *Ji'nan* 250013, *Shandong*, *China*

Composition, tectonic framework, and evolution of the Luxi Orogenic Belt in the North China Craton during the Late Neoarchean

Abstract: ［**Objective**］The growth and evolution of the early Earth's crust are hot topics in Precambrian research. As one of the oldest cratons in the world, the North China Craton (NCC) has undergone a complex cratonization process accompanied by crustal growth and reworking. ［**Methods**］Existing petrological, geochemical, chronological, and structural geological studies are summarized to reveal the tectonic evolution of the Luxi granite–greenstone belt in the eastern NCC. ［**Results**］Multiple lines of evidence indicate late Neoarchean crustal growth, including continental arc and arc magmatic rocks represented by the Feicheng–Tengzhou magmatic arc and late Neoarchean volcanic rocks, post-collisional crustal-derived magmatism represented by the Lushan–Yishui magmatic belt, sedimentation in a back-arc basin defined by late Neoarchean metamorphic sedimentary rocks, and the strike-slip shear deformation caused by the oblique convergence of plates. The >2.60 Ga tonalite, trondhjemite, granodiorite (TTG) suite and the supracrustal rock belt exposed in the central part of the Luxi area represent an ancient microcontinent with apparent affinity to the Jiaoliao Block. ［**Conclusions**］Therefore, the Luxi granite–greenstone belt is an accretionary orogenic belt located on the western margin of the Jiaoliao Block, namely the Luxi Orogenic Belt. High-angle oblique arc-continent collision and underplating of large volumes of mantle-derived magma represent two crustal growth modes in horizontal and vertical directions, respectively. This orogenic belt has undergone multi-stage evolution, including the formation of initial oceanic crust, subduction, and intracontinental extension from the Neoarchean to the end of the Paleoproterozoic. ［**Significance**］In the late Neoarchean, extensive crustal growth occurred around the Jiaoliao Block in the eastern NCC, which was controlled by an early plate

基金项目：国家自然科学基金项目（41872225, 4197021373, 42302260）；福建省自然科学基金项目（2023J01962, 2024J01848）

This research was financially supported by the National Natural Science Foundation of China (Grant Nos. 41872225, 4197021373, and 42302260), and the Natural Science Foundation of Fujian Province (Grant Nos. 2023J01962 and 2024J01848).

第一作者：王东明（1984—），男，博士，讲师，从事早前寒武纪大陆构造变形研究。Email：wdmlittleF@163.com

通信作者：胡健民（1959—），男，博士，研究员，从事构造地质学与区域地质学研究。Email：jianminhu@vip.sina.com

收稿日期：2025−03−28；**修回日期**：2025−09−04；**录用日期**：2025−09−04；**网络出版日期**：2025−09−04；**责任编辑**：范二平

Received：2025−03−28；Revised：2025−09−04；Accepted：2025−09−04；Available Online：2025−09−04；Handling Editor：FAN Erping

tectonic regime characterized by hot subduction.

Keywords: accretionary orogenic belt; late Neoarchean; crustal accretion mechanisms; North China Craton; early plate tectonics

摘　要：地球早期地壳的增生和演化是早前寒武纪研究的核心科学问题。华北克拉通作为全球最古老的克拉通之一，新太古代晚期（2.50～2.48 Ga）经历了复杂的克拉通化过程并伴随强烈的地壳增生和改造。鲁西花岗–绿岩带位于华北克拉通东部，已有的岩石学、地球化学、年代学和构造变形研究显示，鲁西地区发育一系列指示新太古代晚期地壳增生的证据，包括以肥城–滕州岩浆弧和新太古代晚期变质火山岩为代表的陆缘弧和岛弧岩浆岩、以鲁山–沂水岩浆岩带为代表的后碰撞壳源岩浆记录、新太古代晚期变沉积岩所代表的弧后盆地沉积以及板块斜向汇聚导致的大型走滑剪切变形。出露于鲁西地区中部的>2.60 Ga的英云闪长岩、奥长花岗岩、花岗闪长岩（TTG岩系）和表壳岩组合代表一个与胶辽地块具有明显亲缘性的古老陆块。因此，鲁西花岗–绿岩带是一个位于胶辽地块西缘的增生型造山带，即鲁西造山带。弧–陆高角度斜向碰撞和巨量幔源岩浆底垫分别代表了胶辽地块西缘水平和垂向地壳增生。该造山带在新太古代到古元古代末期经历了初始洋壳形成、俯冲到陆内伸展等构造演化阶段。新太古代晚期，华北克拉通东部胶辽地块周缘发生了广泛的地壳增生作用，这一过程受控于以板块热俯冲为特征的早期板块构造体制。

关键词：增生造山带；新太古代晚期；地壳增生机制；华北克拉通；早期板块构造

中图分类号：P548　　**文献标识码：**A　　**文章编号：**1006−6616(2026)02−0285−27

DOI：10.12090/j.issn.1006-6616.2025033

0　引言

造山作用是指在地球深部动力学背景下岩石圈发生剧烈构造变动和物质重组的地质过程，涉及强烈的变形、变质及岩浆作用，是研究地壳形成、演化及其动力学体制的关键地带（Dewey et al., 2021; Ghosh et al., 2022; Lu et al., 2023）。依据造山带内部的构造单元类型及其构造属性，造山带可划分为增生型、碰撞型和陆内造山带3种类型。其中增生型造山带是由大洋岩石圈长期俯冲、增生形成的宽阔造山带（Condie, 2007; Cawood et al., 2009），包括增生楔、俯冲和上冲板块残片、岛弧和弧后组合、蛇绿岩、洋底高原、外来陆块、与俯冲有关的岩浆活动、局部超高压–超高温变质以及沉积盆地（Cawood et al., 2009; 肖文交等, 2019）。

增生型造山作用是地壳增生的重要机制（Santosh et al., 2010; Safonova and Santosh, 2014; Xiao and Santosh, 2014; Safonova, 2017），目前研究认为地壳增生方式包括新生大洋岛弧、洋底高原和增生杂岩的水平侧向增生以及岩浆底垫导致的陆壳垂向增生（Kemp et al., 2009; Safonova and Santosh, 2014）。由于前寒武纪期间产生巨量的新生陆壳，所以相比较显生宙而言具有更高的陆壳增生速率（Santosh et al., 2013）。很多学者认为早前寒武纪陆壳增生过程为早期板块构造体制下汇聚板块边界的弧−弧碰撞或弧−陆碰撞，陆壳增生时期主要集中在太古代—古元古代（Zhai and Santosh, 2011; Oliveira et al., 2011; Korsch et al., 2011; Rojas-Agramonte et al., 2011）。前寒武纪期间陆块之间的洋盆俯冲、闭合为地壳强烈增生改造提供了必要的地球动力学条件（Condie, 2005; Cawood et al., 2013; Perchuk et al., 2018; Brown et al., 2020），并且前寒武纪早期增生造山带内部发育的岩浆、变质、沉积作用和构造变形组合与显生宙造山带类似，也具有相似的垂向和水平陆壳增生过程（Cawood et al., 2018; Kusky et al., 2018）。

华北克拉通是具有>3.80 Ga陆核的古老陆块（Liu et al., 1992; Wan et al., 2023），新太古代晚期（约2.50 Ga）的克拉通化过程表现为微陆块通过绿岩带发生碰撞拼贴（Zhai, 2014; Zhai and Santosh, 2011; Bao et al., 2022）。鲁西地区是华北克拉通太古宙基底出露最为完整的地区之一。综合分析已有的岩石学、地球化学、年代学和构造学研究成果（曹国权等, 1996; Wang et al., 2013b）表明，以往所谓的鲁西花岗−绿岩带实际是一个新太古代晚期的增生造山带。新太古代晚期这个造山带内发生了以弧−陆斜向汇聚为特征的块体拼贴和垂向的幔源岩浆底垫，是华北克拉通东部新太古代晚期的增生造山作用典型代表。这一观点为认识华北克拉通新太古代晚期地壳演化机制提供了思路和依据。

1　区域地质背景

1.1　华北克拉通早前寒武纪构造格架

华北克拉通太古宙基底可划分为胶辽、迁怀、鄂尔多斯、集宁、许昌、徐淮和阿拉善 7 个微陆块（Zhai and Santosh, 2011），微陆块之间低级变质的花岗–绿岩带代表洋盆闭合的拼贴带。新太古代晚期（2.55～2.48 Ga），华北克拉通发生广泛的陆壳增生改造事件并伴随强烈构造–岩浆–变质作用（Gao et al., 2021; He et al., 2021; Liou et al., 2022; Diwu et al., 2024），代表了微陆块之间的洋壳俯冲及弧–陆碰撞或陆–陆碰撞的克拉通化过程（Zhai et al., 2005; Zhai and Santosh, 2011; Santosh et al., 2016）。太古宙绿岩带包括集宁和迁怀地块之间的遵化绿岩带、鄂尔多斯地块与迁怀地块之间的五台山绿岩带、集宁和鄂尔多斯地块之间的东五分子绿岩带、胶辽和迁怀地块之间的雁翎关绿岩带、许昌和鄂尔多斯地块之间的登封绿岩带（图 1）。除雁翎关绿岩带形成于 2.7～2.8 Ga，并被 2.7 Ga 英云闪长岩、奥长花岗岩和花岗闪长岩（TTG 岩系）侵入外（Polat et al., 2006; Cheng and Kusky, 2007），其余绿岩带均形成于新太古代晚期。绿岩带由含条带状硅铁建造（BIF）的火山–沉积岩组成，代表陆块间边缘海沉积，下部为双峰式火山岩与少量科马提岩互层，上部为钙碱性火山岩及大理岩组合（翟明国等，2020）。五台山、雁翎关及遵化绿岩带中部分变玄武岩可见枕状构造，变沉积岩多为变砂岩、变泥质岩及 BIF。绿岩带内变玄武岩多数具有岛弧玄武岩地球化学特征，部分具有弧后玄武岩亲缘性，少数具有洋中脊玄武岩特征（Zhao et al., 2007; Wang, 2009; Zhai, 2014; Fu et al., 2021; He et al., 2021; Wang et al., 2022），暗示新太古代晚期板块俯冲背景下强烈的壳幔相互作用及陆壳物质循环。

1.2　鲁西地区早前寒武纪地质背景

1.2.1　区域构造格架

鲁西地区位于华北东部。呈北西向展布的太古宙基底岩系构成了一条典型的花岗–绿岩带（曹国权等，1996），代表胶辽地块与迁怀地块的碰撞拼合带（Zhai and Santosh, 2011）。太古宙岩石主要由 TTG 片麻岩、花岗岩及表壳岩组成。其中新太古代晚期侵入岩广泛发育，约占总面积的 85% 以上；表壳岩呈透镜状或条带状出露于花岗岩或 TTG 片麻岩中（图 2）。鲁西地区在约 2.70 Ga 发生了巨量地壳增生，随后在 2.60 Ga、2.50 Ga 发生强烈的地壳增生和改造（Wan et al., 2010, 2011; Ren et al., 2016;

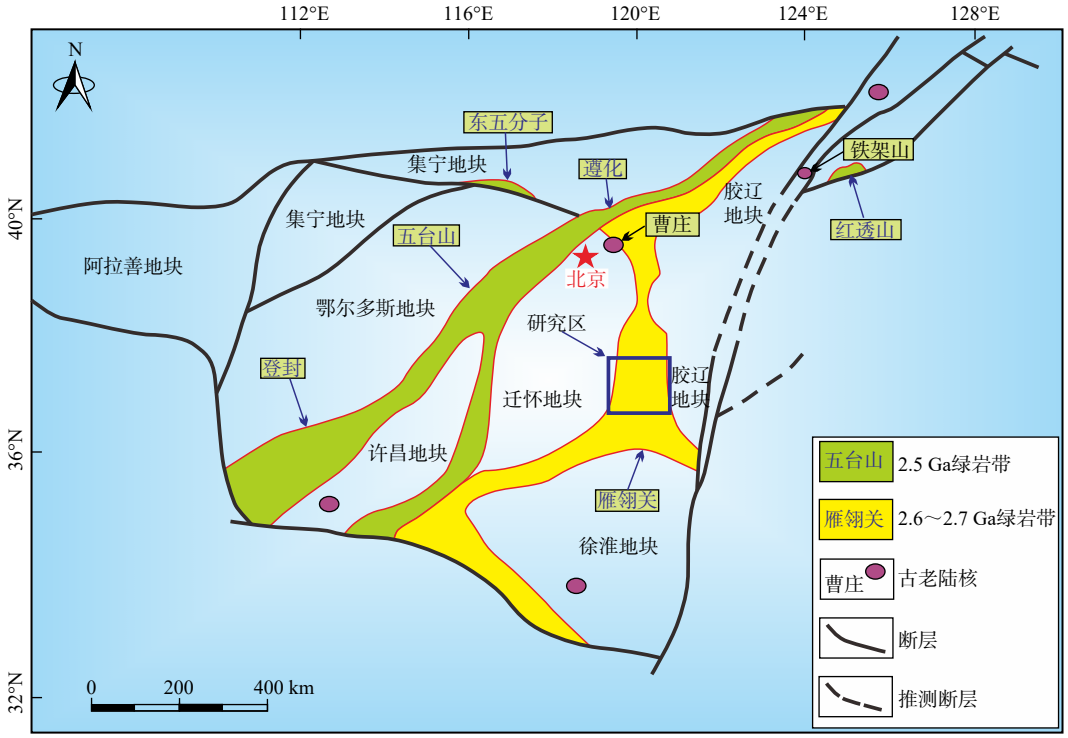


图 1　华北克拉通基底构造单元划分（Zhai and Santosh，2011）

Fig. 1　Tectonic subdivision of the North China Craton basement (modified after Zhai and Santosh, 2011)

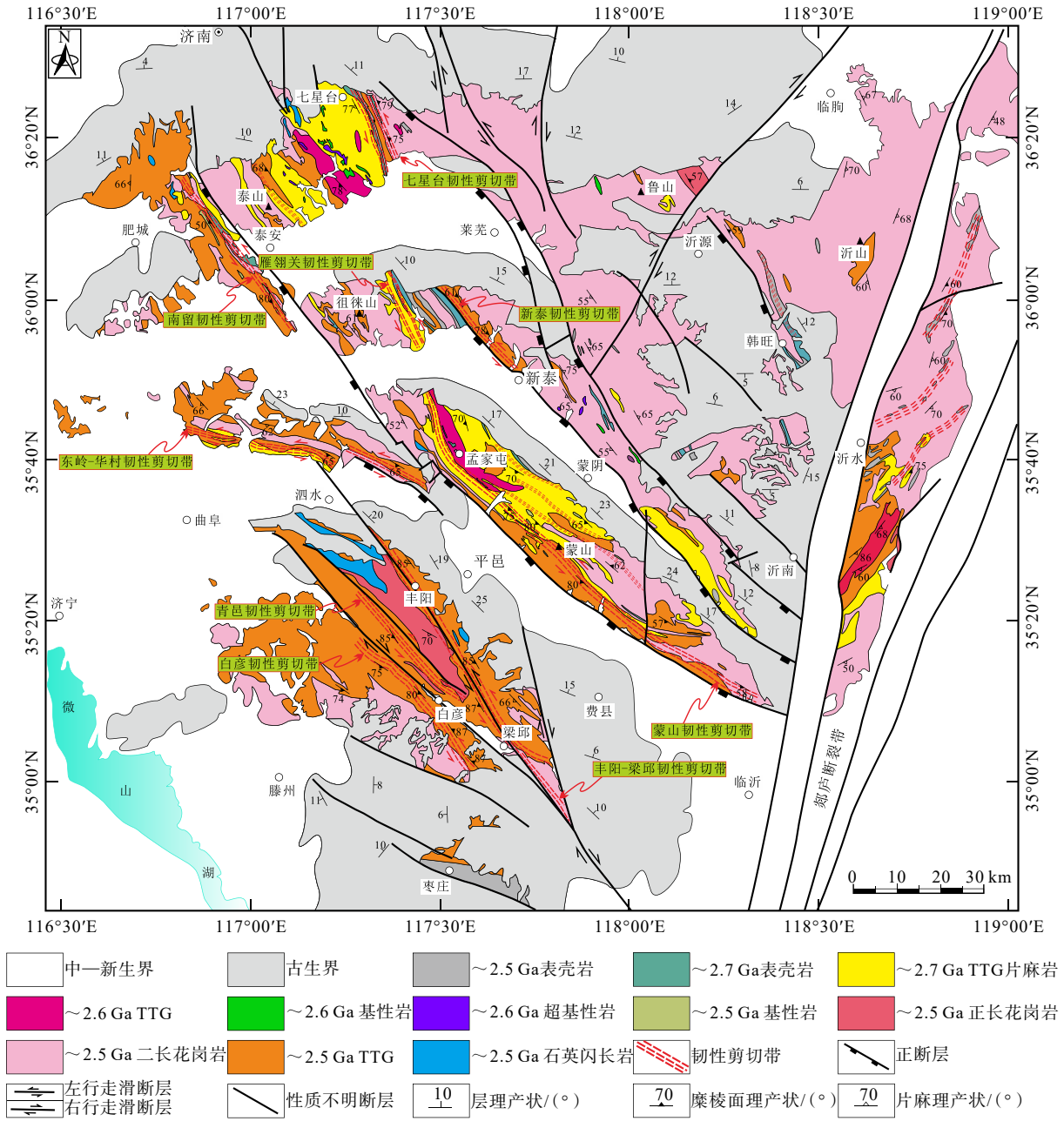


图 2 鲁西地区地质简图（山东省地质调查院，2021）

Fig. 2 Simplified geological map of the Luxi area (modified after Shandong Institute of Geological Survey, 2021)

Yakymchuk et al., 2019)。

1.2.2 侵入岩岩浆演化序列

新太古代早期(2.75～2.70 Ga)侵入岩以 TTG 片麻岩为主，岩石因遭受强烈的深熔作用而具有条带状构造(陆松年等, 2008; Wan et al., 2011)。这一期岩浆活动具有亏损地幔源区的特点，并伴随少量古老陆壳物质的再循环，代表华北克拉通东部乃至全球范围内重要地壳增生事件(Wan et al., 2011, 2014a; Wang et al., 2025)。

新太古代中期(约 2.60 Ga)岩浆岩呈捕虏体形式产出于 2.50 Ga 花岗岩中。岩石类型较为复杂，包括变镁铁质–超镁铁质岩、TTG 片麻岩和片麻状花岗岩等(Ren et al., 2016; 王伟等, 2016; Yakymchuk et al., 2019; 万渝生等, 2019)，代表地幔柱或地幔翻转背景下、有流体参与的部分熔融事件，形成于软流圈上涌的伸展构造体制(Ren et al., 2016; Yakymchuk et al., 2019)。鲁西地区尚未发现约 2.60 Ga 的表壳岩组合(Wan et al., 2014b)。

新太古代晚期是华北克拉通陆壳增生、改造的重要时期(Wang and Liu, 2012; Diwu et al., 2024)。鲁

西地区新太古代晚期侵入岩主要由 2.55～2.50 Ga 二长花岗岩、正长花岗岩以及 TTG 岩石组成(Wan et al., 2012b; Wang et al., 2017b; Sun et al., 2019a; Shi et al., 2019)。接触关系、锆石 U-Pb 定年、Nd-Hf 同位素显示，新太古代晚期岩浆岩为古老片麻岩深熔后经过分离结晶形成，暗示中太古代晚期—新太古代早期的陆壳再造和活化(Wan et al., 2011)。

1.2.3　表壳岩系时空演化

新太古代表壳岩包括泰山岩群、孟家屯岩组和济宁岩群(图 3)。以往研究将泰山岩群划分为雁翎关岩组、柳杭岩组和山草峪岩组 3 个岩石构造单元(曹国权等, 1996)。

雁翎关岩组主要由斜长角闪岩、黑云角闪片麻岩以及具有鬣刺结构的科马提岩组成(Polat et al., 2006; Cheng and Kusky, 2007)，形成时代为 2.75～2.74 Ga(Wan et al., 2011)。柳杭岩组下段以变枕状玄武岩为主，上段由细粒黑云片麻岩和变质砾岩组成。在七星台地区，由侵入柳杭岩组的片麻状奥长花岗岩以及变质玄武岩中变安山岩夹层的锆石 U-Pb 测年限定柳杭岩组下段变玄武岩形成年龄为 2.74～2.71 Ga(Wang et al., 2013b)，上段的变沉积岩年龄为 2.53 Ga(Wan et al., 2012a)。山草峪岩组主要由细粒黑云片麻岩夹斜长角闪片岩、细粒角闪黑云片麻岩、细粒二云片麻岩及黑云片岩组成，局部残留的沉积构造表明其原岩为碎屑岩(Wan et al., 2012a)。孟家屯岩组主要由石榴石英岩、石英云母片岩、斜长角闪岩及少量细粒片麻岩组成，原岩为大陆边缘古岛弧环境下的拉斑玄武岩与陆源碎屑岩沉积，沉积时代为 2.72～2.70 Ga，并在 2.64～2.60 Ga 经历绿片岩相–角闪岩相变质(陆松年等, 2008)。济宁岩群是鲁西地区 BIF 铁矿重要的赋矿层位，但地表未见出露。钻孔揭露岩性主要为绢云千枚岩、板岩和 BIF，原岩为钙质泥岩、含火山岩砾石的粉砂质泥岩、中酸性熔岩及凝灰岩，变质程度明显低于泰山岩群(Wan et al., 2012a)。Wan et al.(2012a)获得济宁岩群长英质火山岩时代为 2.56 Ga，而非以往认为的古元古代。综上可知，鲁西地区新太古代表壳岩可划分为两部分(Wan et al., 2012a; 王伟等, 2016)：① 新太古代早期(2.75～2.70 Ga)雁翎关–柳杭岩系，包括泰山岩群的雁翎关岩组和柳杭岩组下段的基性—超基性火山岩和孟家屯岩组陆源碎屑岩。②新太古代晚期(2.56～2.53 Ga)山草峪–济宁岩系，包括山草

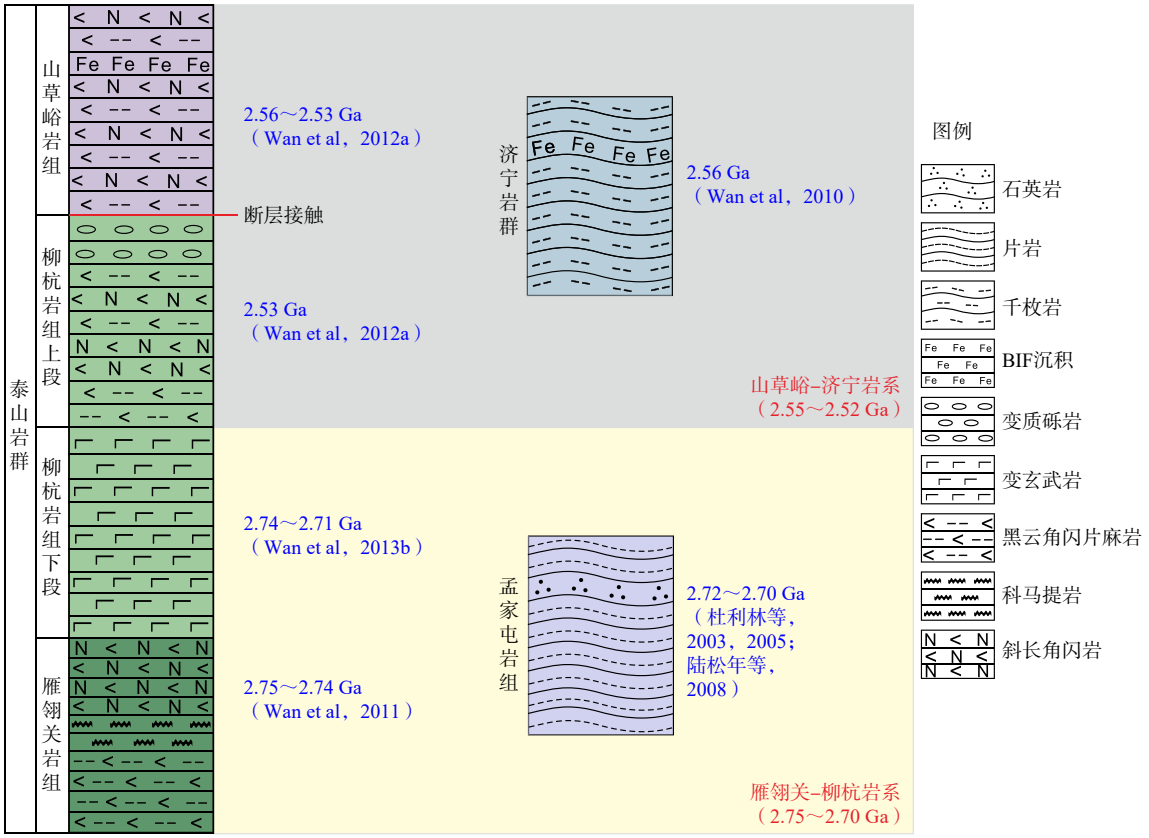


图 3　鲁西地区新太古代表壳岩地层柱状示意图

Fig. 3　Stratigraphic column of the Neoarchean supracrustal rocks in the Luxi area

峪岩组、柳杭岩组上段和济宁岩群，主要由细粒黑云片麻岩、砾岩、BIF 和长英质火山岩组成（图 3）。

依据形成时代和岩性组合，鲁西地区太古宙基底可划分为 A、B、C 3 个岩性带，分别为北东侧 A 岩性带 2.52～2.48 Ga 壳源花岗岩带，中部 B 岩性带 2.75～2.60 Ga TTG 片麻岩和表壳岩古老岩石带，南西侧 C 岩性带 2.56～2.53 Ga 闪长岩、石英二长闪长岩和花岗闪长岩（Wan et al., 2010; Gao et al., 2018; Hu et al., 2019a, 2019b; Sun et al., 2019a, 2019b）。A 岩性带壳源花岗岩侵入 B 岩性带和 C 岩性带。

2 新太古代晚期活动陆缘岩浆作用

2.1 陆缘弧侵入岩

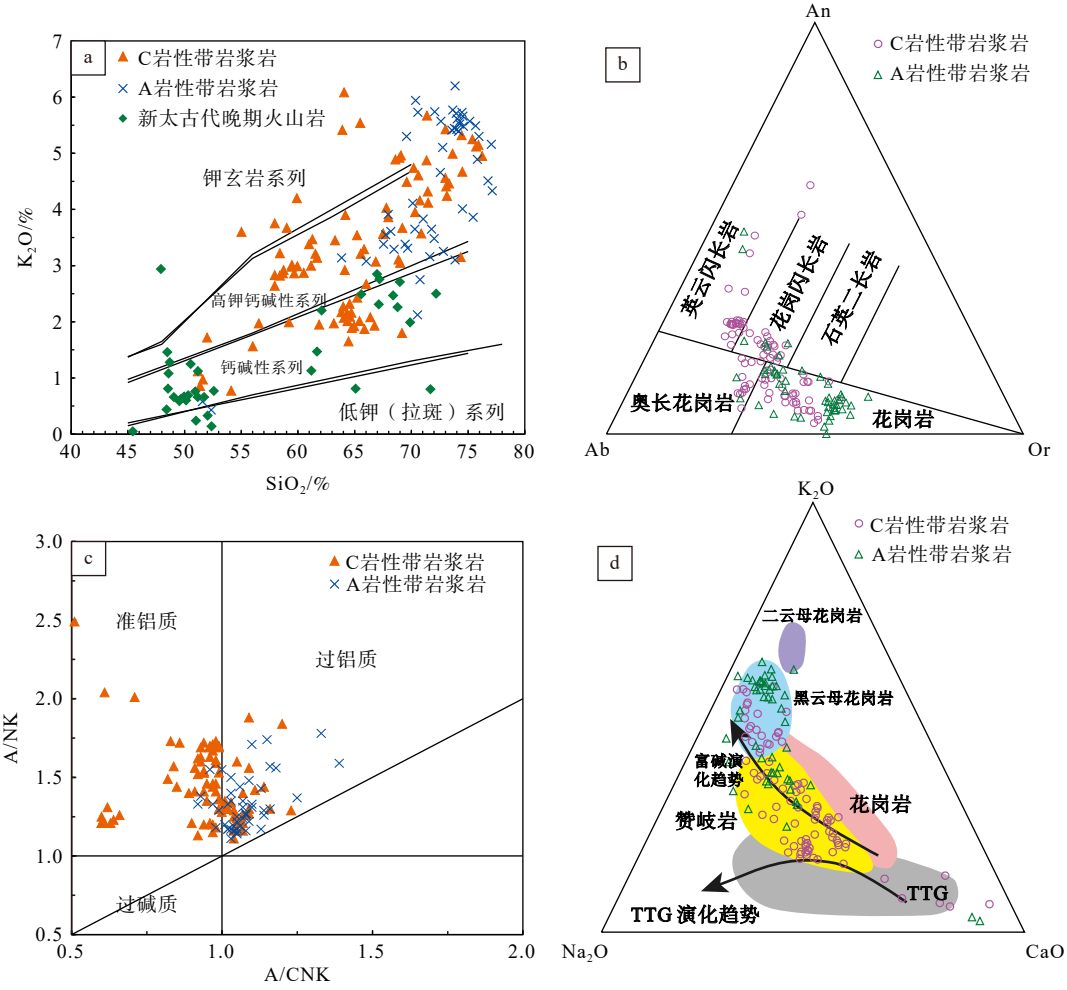
鲁西地区 C 岩性带为一条 2560～2530 Ma 岩浆岩带，岩性主要为闪长岩、石英闪长岩和花岗闪长岩，以钙碱性—高钾钙碱性岩系为主（图 4a）。An-Ab-Or 三角分类图解中多落于花岗岩、花岗闪长岩区（图 4b），具有准铝质—过铝质特点（图 4c）；K_2O-Na_2O-CaO 三角图解中样品显现出明显的由 TTG 向黑云母花岗岩的演变趋势（图 4d）。稀土配分曲线显示右倾特征，具明显 Eu 负异常（图 5a），原始地幔标准化微量元素蛛网图显示 Nb、Ti 亏损，而富集 Zr、Hf、Th 和 U（图 6a）。Th/Yb-Ta/Yb 判别图解中样品全部落于活动大陆边缘（陆缘弧）区域及其附近（图 7a），MgO-SiO_2 图解和 TiO_2-MgO 图解显示岩石具有埃达克岩和低 Ti 赞岐岩的地球化学特征（图 7b、7c）。Nb/Ta-Zr/Hf 图解显示鲁西地区新太古代晚期岩浆作用具有连续的演化趋势（图 7d），说明岩浆形成于统一、连续的板块俯冲过程且受控于部分熔融过程（Yu et al., 2021）。埃达克岩可能来源于俯冲洋壳的部分熔融或埃达克质母岩浆与上覆地幔楔之间的相互作用（Peng et al., 2012）。赞岐岩的高 $Mg^{\#}$、Cr、Sr、Ba、K_2O/Na_2O 特征指示板块俯冲背景下壳幔岩浆混合（Sun et al., 2019a）。高 K 花岗岩表现出以中地壳层次硬砂岩部分熔融的源区特征（Gao et al., 2018; Hu et al., 2019a），部分 TTG 片麻岩为下地壳镁铁质岩石部分熔融的产物（图 7e）。全岩 Nd 同位素和岩浆锆石 Hf 同位素数据点多数落于球粒陨石和亏损地幔演化线之间，个别样品 $\varepsilon_{Hf}(t)$ 为负值，落于球粒陨石演化线下方（图 8a、8b）。综上，C 岩性带为与新太古代晚期洋壳俯冲有关的活动大陆边缘的岩浆弧，证实了在 2.56～2.53 Ga 期间鲁西地区发生强烈的壳幔相互作用及地壳增生（Wang et al., 2009; Peng et al., 2012; Sun et al., 2019a; Hu et al., 2019a）。

2.2 后碰撞壳源岩浆活动

鲁西地区 A 岩性带以富钾二长花岗岩和正长花岗岩为主（Wan et al., 2010），岩石多为高钾钙碱性—钾玄岩系（图 4a）。在 An-Ab-Or 分类图解中样品点落于花岗岩区（图 4b），多具有过铝质特征（图 4c）；在 K_2O-Na_2O-CaO 三角图解中样品多落于黑云母花岗岩区（图 4d）。稀土配分曲线形态与肥城–滕州岩浆弧相似，显示轻稀土富集的右倾形态（图 5b）。微量元素蛛网图显示 Nb、Ti、P 亏损，而 Zr、Hf 富集（图 6b）。在 Th/Yb-Ta/Yb 岩石成因判别图解中样品全部落于活动大陆边缘区（图 7a）；MgO-SiO_2 判别图解和 TiO_2-MgO 赞岐岩判别图解显示其具有高 Si 埃达克岩和低 Ti 赞岐岩的特征（图 7b、7c），指示活动大陆边缘构造背景。岩浆锆石 Hf 同位素数据绝大多数落于球粒陨石和亏损地幔演化线之间，部分样品点位于球粒陨石演化线下方（图 8a）；全岩 Nd 同位素与 Hf 同位素具有相似的特点，个别样品点落于球粒陨石下方（图 8b）。岩浆源区判别图解显示富钾壳源花岗岩主要由变质杂砂岩部分熔融形成（图 7e），并导致早期岩石发生变质–深熔作用（Wang et al., 2017b）。2.54～2.49 Ga 岩浆岩未变形的块状构造、代表伸展构造背景的镁铁质岩墙（Gao et al., 2019b; Liu et al., 2019）与稳定的 BIF 沉积（Wan et al., 2012a; Wang et al., 2014），暗示在 2.54 Ga 鲁西地区的构造体制由挤压向伸展转变，富钾壳源花岗岩代表弧–陆碰撞后软流圈上涌导致地壳部分熔融事件，伴随小规模幔源镁铁质岩浆活动（Yu et al., 2019, 2021; Gao et al., 2019a, 2019b）。

2.3 岛弧火山岩

鲁西地区 2.56～2.53 Ga 中酸性火山岩多为钙碱性岩系，少数样品落于拉斑玄武岩区（图 4a）。稀土配分曲线显示 2 种类型，其一为右倾，其二具有平缓形态（图 5c、5d），分别对应 Condie（1981）划分的 TH1 和 TH2 这 2 种类型。TH1 型微量元素蛛网图表现较为平坦形态，Ti、Nb 亏损程度明显低于 TH2 型，其 La/Yb、Th/Yb 和 Nb/Yb 比值接近于正常型洋中脊玄武岩（N-MORB），指示其地幔源区没有受到明显的外来物质的扰动，即软流圈地幔的低压部分熔融（刘树文等，2021）。TH2 型更富集 Rb、Sr、Zr、Hf（图 6c、6d），具有更高的 La/Yb、Nb/Yb 比值。二者分别形成于弧后盆地或大洋盆地和岛弧–大陆



新太古代晚期火山岩数据引自 Wang et al.(2013c)、Gao et al.(2020)；C 岩性带岩浆岩数据引自 Sun et al.(2019a, 2020)、Wang et al.(2017b)、Peng et al.(2012)、Yu et al.(2021)；A 岩性带岩浆岩数据引自 Wang et al.(2017b)、Wan et al.(2012b)、Gao et al.(2018)、Sun et al.(2020)

a—SiO_2-K_2O 分类图解(Laurent et al., 2013)；b—An-Ab-Or 分类图解(O'Connor, 1965)；c—A/NK-A/CNK 图解(Maniar and Piccoli, 1989)；d—K_2O-Na_2O-CaO 三角图解(Moyen et al., 2003)

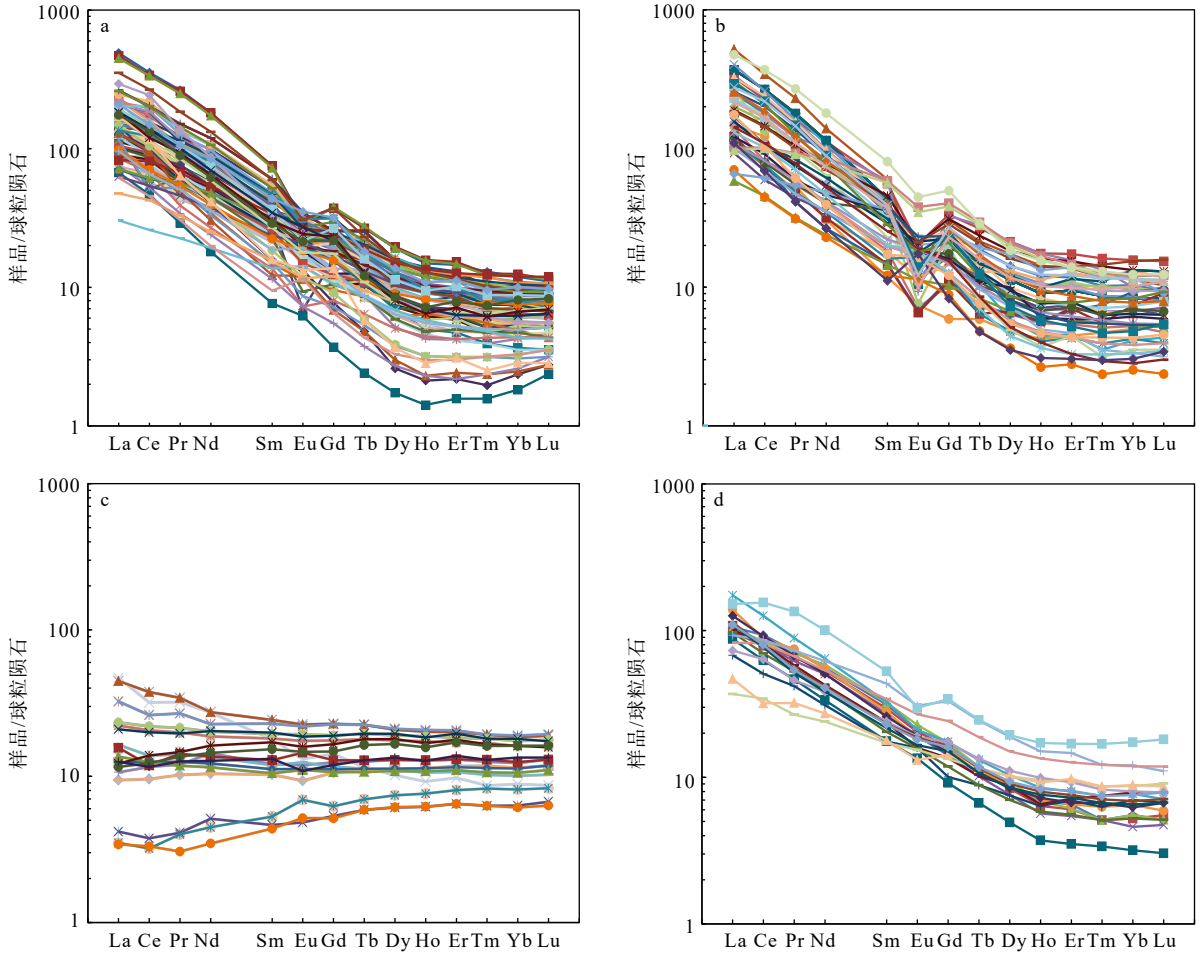
图 4　地球化学分类图解

Fig. 4　Geochemical classification diagrams

(a) K_2O versus SiO_2 diagram (Laurent et al., 2013); (b) An versus Ab versus Or diagram (O'Connor, 1965); (c) A/NK versus A/CNK diagram (Maniar and Piccoli, 1989); (d) K_2O versus Na_2O versus CaO diagram (Moyen et al., 2003).

Data on late Neoarchean volcanic rocks are cited from Wang et al., 2013c, Gao et al., 2020. Data on magmatic rocks in the C belt are cited from Sun et al., 2019a, 2020, Wang et al., 2017b, Peng et al., 2012, Yu et al., 2021. Data on magmatic rocks in the A Belt are cited from Wang et al., 2017b, Wan et al., 2012b, Gao et al., 2018, Sun et al., 2020.

边缘构造环境(Zhai and Santosh, 2011)。在 Th/Yb-Ta/Yb 岩石成因判别图解中样品全部落于活动大陆边缘区(图 7a)，具有埃达克岩和赞岐岩的地球化学特征(图 7b、7c)，说明鲁西地区约 2.50 Ga 火山岩为岛弧拉斑−钙碱性火山岩。岩浆锆石 Hf 同位素数据点多数落于亏损地幔和球粒陨石演化线之间，少部分样品点落于亏损地幔上方和球粒陨石线下方(图 8a)，全岩 Nd同位素数据点多数落于亏损地幔和球粒陨石演化线之间，少数样品位于亏损地幔演化线上方(图 8b)。岩浆主要来源于被流体或熔体交代的亏损地幔或俯冲板片的部分熔融，又或是拆离的下地壳的部分熔融(图 7e; Wang et al., 2009; Wang et al., 2013c; Gao et al., 2020; Yang et al., 2020)。也有学者在鲁西地区识别出与俯冲板片后撤有关的高 Mg 安山岩，具有与显生宙玻镁安山岩类似的地球化学特征，源区经历过早期玄武质岩浆的抽离和随后的俯冲交代作用(Peng et al., 2013)，也间接说明了新太古代晚期板块发生水平位移，洋壳碎片或地幔



a—C 岩性带岩浆岩球粒陨石标准化稀土元素配分曲线；b—A 岩性带岩浆岩球粒陨石标准化稀土元素配分曲线；c—新太古代晚期 TH1 型火山岩球粒陨石标准化稀土元素配分曲线；d—新太古代晚期 TH2 型火山岩球粒陨石标准化稀土元素配分曲线（TH1 和 TH2 类型火山岩的分类方法据 Condie et al.（1981））

图 5 球粒陨石标准化稀土元素配分曲线（数据来源同图 4）

Fig. 5 Chondrite-normalized REE patterns (data sources are the same as in Fig. 4)

(a) Chondrite-normalized REE patterns for magmatic rocks of the C belt; (b) Chondrite-normalized REE patterns for magmatic rocks of the A belt; (c) Chondrite-normalized REE patterns for late Neoarchean TH1-type volcanic rocks; (d) Chondrite-normalized REE patterns for late Neoarchean TH2-type volcanic rocks. The classification of TH1 and TH2 volcanic rocks is based on Condie et al., 1981.

楔等侧向拼贴于活动大陆边缘。所以，鲁西地区肥城–滕州岩浆弧和新太古代末火山岩的岩浆源区均有被流体或熔体交代的地幔物质加入（Sun et al., 2019a; Yang et al., 2020; Yu et al., 2021），并伴随少量下地壳镁铁质岩石部分熔融（Hu et al., 2019a），代表了新太古代晚期洋壳俯冲过程中的岛弧、陆缘弧岩浆，与地壳重熔的花岗岩差别明显。

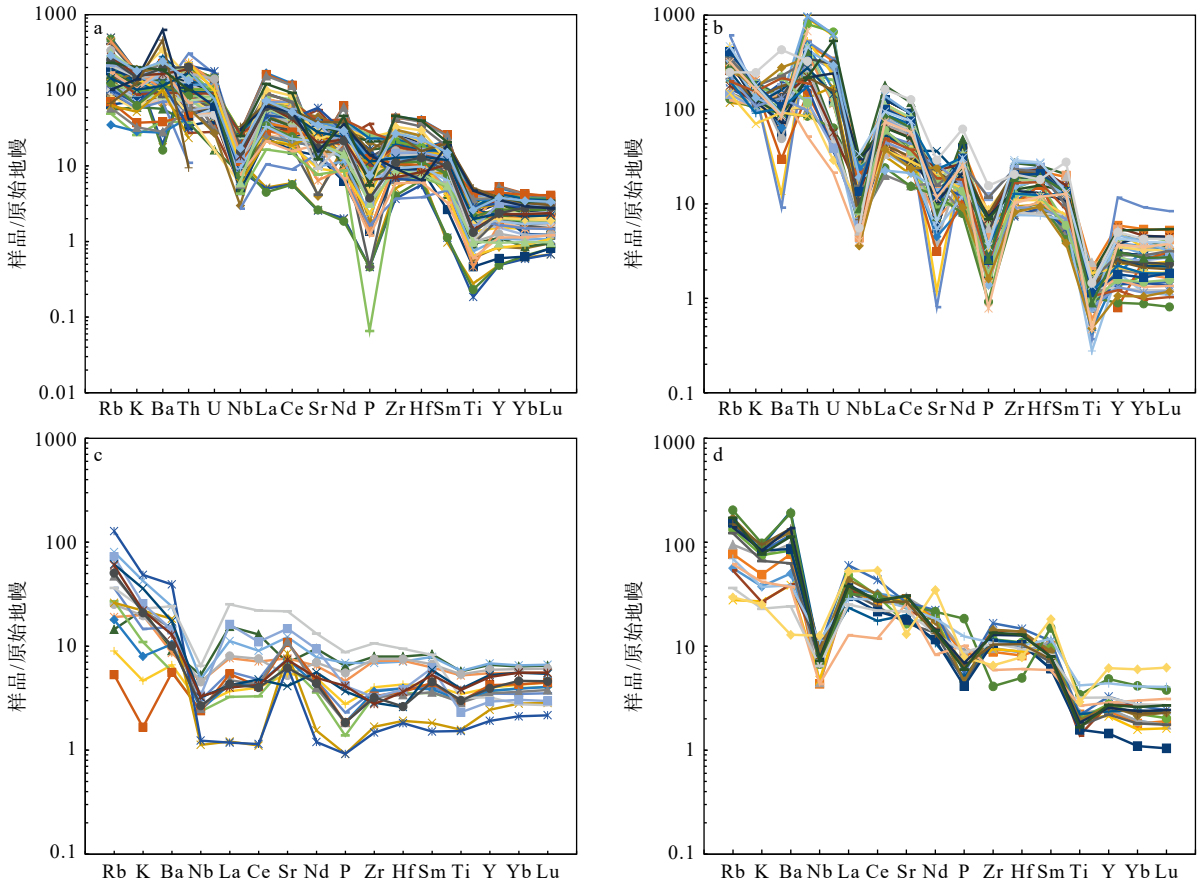
3 新太古代晚期岛弧盆地沉积

3.1 岩性和沉积相特征

鲁西地区新太古代表壳岩可划分为 2 部分，下部为>2.70 Ga 基性—超基性火山岩，上部为 2.55～2.50 Ga 火山–沉积岩（Wan et al., 2012a; Wang et al., 2014）。后者主要包括柳杭岩组上段、山草峪岩组和济宁岩群，原岩主要为浅海相碎屑岩夹中酸性火山岩。

山草峪岩组大致可分为 3 个岩性段，下部以含石榴石细粒黑云片麻岩为主；中段以细粒黑云片麻岩及含铁石英岩为主；上段由细粒黑云片麻岩、黑云片岩及 BIF 组成；与雁翎关和柳杭岩组呈断层接触（图 9）。

中上段发育粒序层理，局部见斜层理。每个沉积韵律层自下而上表现为石英含量由多变少、粒度变细、黑云母由少变多。反映下部以砂级碎屑为



a—C 岩性带岩浆岩原始地幔标准化微量元素蛛网图；b—A 岩性带岩浆岩原始地幔标准化微量元素蛛网图；c—新太古代晚期 TH1 型火山岩原始地幔标准化微量元素蛛网图；d—新太古代晚期 TH2 型火山岩原始地幔标准化微量元素蛛网图（TH1 和 TH2 类型火山岩的分类方法据 Condie et al.（1981））

图 6　原始地幔标准化微量元素蛛网图（数据来源同图 4）

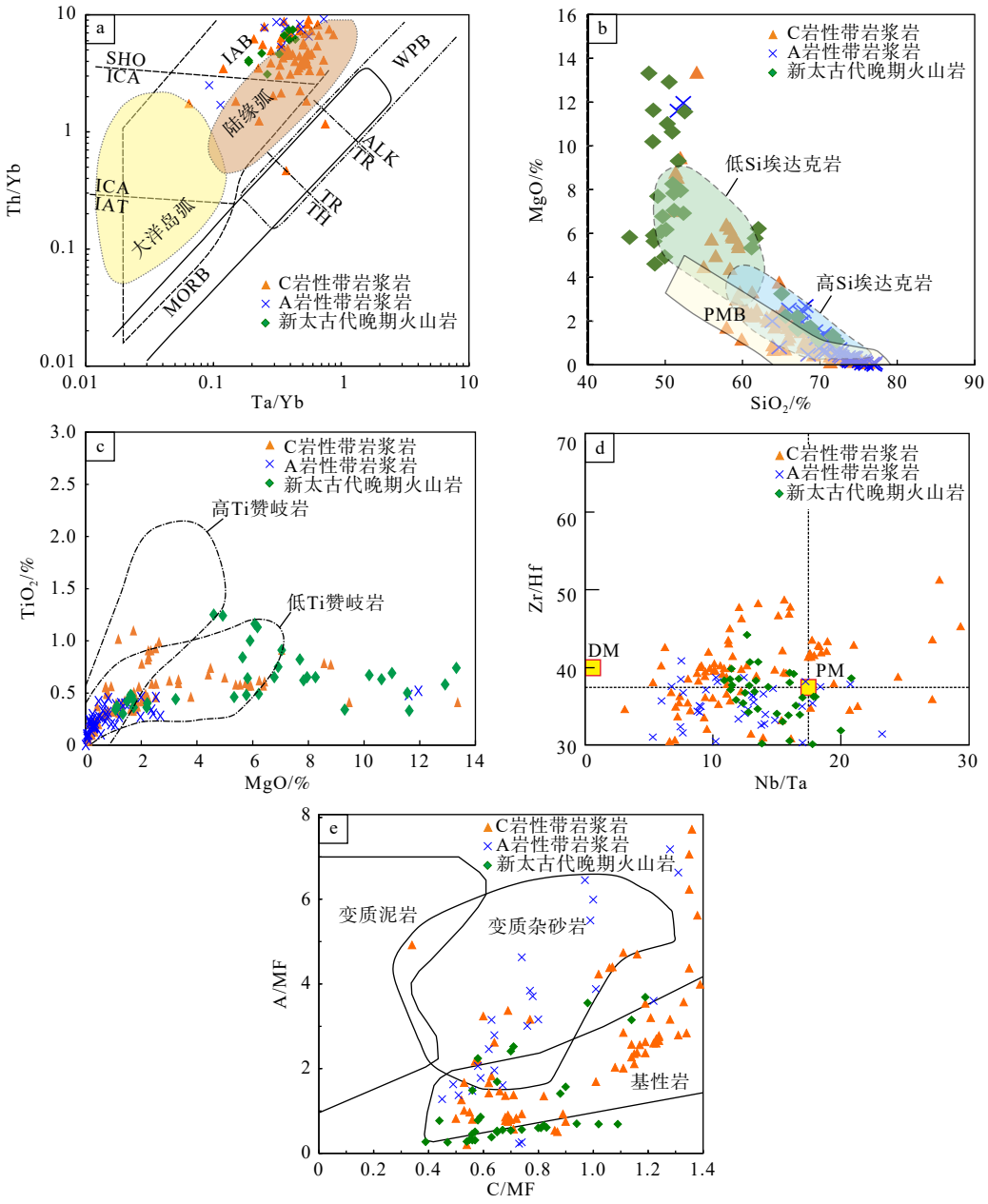
Fig. 6　Primitive mantle normalized diagrams for whole rock (data source is the same as for Fig. 4)

(a) Primitive mantle-normalized spider diagrams for magmatic rocks of the C belt; (b) Primitive mantle-normalized spider diagrams for magmatic rocks of the A belt; (c) Primitive mantle-normalized spider diagrams for late Neoarchean TH1-type volcanic rocks; (d) Primitive mantle-normalized spider diagrams for late Neoarchean TH2-type volcanic rocks. The TH1 and TH2 volcanic rock classification is based on Condie et al. (1981).

主，向上泥质增多。细粒片麻岩具变余砂状结构和凝灰质粉砂结构，片岩具变余泥质粉砂结构和层理构造，顶部黑云片岩具变余凝灰结构（山东省地质调查院，2021）。因此，山草峪岩组原岩为粉砂—细砂碎屑岩和硅铁建造，夹中酸性火山岩和凝灰质粉砂岩，属较稳定环境下的浅海相沉积。柳杭岩组下段为蛇纹石片岩、阳起片岩、黑云片岩及斜长角闪岩，原岩为>2.70 Ga 的变玄武岩（Wan et al., 2012a）；上段由片岩、细粒片麻岩及变质砾岩组成，与下段多呈断层接触（图 10）。变质砾岩中砾石主要为中细粒奥长花岗岩，少量石英闪长岩、斜长角闪岩等，呈透镜状和浑圆状，发育沉积韵律。细粒片麻岩及片岩具变余凝灰角砾状结构、凝灰结构和砂状结构，说明原岩为碎屑岩及中酸性火山碎屑岩、凝灰岩（山东省地质调查院，2021）。济宁岩群主要为灰绿色钙质、硅质、铁质千枚岩、千枚状板岩和 BIF，中下部含中酸性火山熔岩和火山碎屑岩（宋明春等，2011）。原岩为一套泥灰岩、砂岩夹酸性火山岩及硅铁沉积建造，属浅海相—深海相泥灰岩、砂岩夹中酸性火山岩及硅铁建造。

3.2　沉积物源分析

山草峪岩组含石榴石副片麻岩具有相对较高的 MgO、FeO^T，暗示镁铁质地壳是山草峪岩组变沉积岩的重要源区。碎屑锆石测年结果显示出 2 个明显年龄峰值，分别为 2.56～2.52 Ga 和 2.72～2.70 Ga，与新太古代侵入岩具有相似的年龄谱图（图 11a、



IAB—岛弧玄武岩；IAT—岛弧拉斑玄武岩；ICA—岛弧钙碱性玄武岩；WPB—板内玄武岩；ALK—碱性玄武岩；TR—过渡玄武岩；TH—拉斑玄武岩；SHO—岛弧橄榄玄粗岩；MORB—大洋中脊玄武岩；N-MORB—正常型洋中脊玄武岩；E-MORB—富集型洋中脊玄武岩；PMB—由玄武岩或角闪岩部分熔融的熔体；PM—原始地幔；DM—亏损地幔

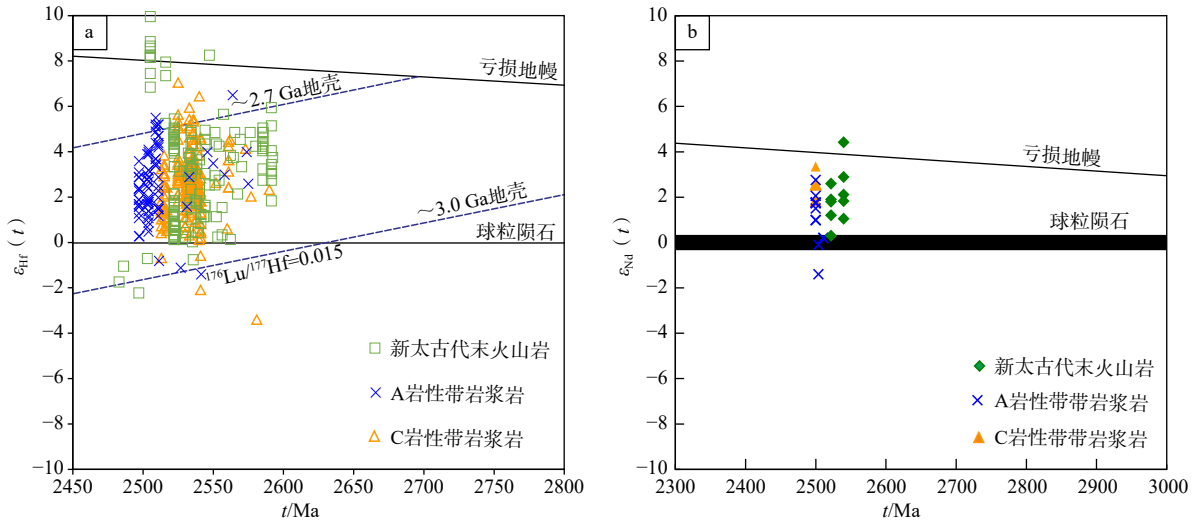
a—Th/Yb-Ta/Yb 判别图解（Pearce, 1983）；b—MgO-SiO_2 判别图解（Martin et al., 2005）；c—Nb/Ta-Zr/Hf 判别图解（数据引自 Mcdonough, 2003）；d—TiO_2-MgO 赞岐岩判别图解（Martin et al., 2009）；e—A/FM-C/FM 岩浆源区判别图解（Altherr et al., 2000）

图 7 岩石成因判别图解（数据来源同图 4）

Fig. 7 Petrogenetic identification diagram (data source is the same as for Fig. 4)

(a) Th/Yb versus Ta/Yb diagram (Pearce, 1983); (b) MgO versus SiO_2 diagram (PMB—melts derived from partial melting of basalt or amphibolite; Martin et al., 2005); (c) Nb/Ta versus Zr/Hf diagram (PM—primitive mantle; DM—depleted mantle, data from Mcdonough, 2003); (d) TiO_2 versus MgO diagram for distinguishing sanukite (Martin et al., 2009); (e) A/FM versus C/FM diagram showing magmatic sources (Altherr et al., 2000)

AT—island arc tholeiite; ICA—island arc calc-alkaline basalt; WPB—within-plate basalt; ALK—alkaline basalt; TR—transitional basalt; TH—tholeiite; SHO—shoshonite; MORB—mid-ocean ridge basalt; N-MORB—normal mid-ocean ridge basalt; E-MORB—enriched mid-ocean ridge basalt.



a—t-$\varepsilon_{Hf}(t)$关系图解（数据引自 Wang et al., 2013c; Guo et al., 2014; Gao et al., 2018, 2020; Sun et al., 2019a, 2020; Yu et al., 2021）；b—t-$\varepsilon_{Nd}(t)$关系图解（数据引自 Jahn et al., 1988; Wang et al., 2013c; Peng et al., 2013; Gao et al., 2018）

图 8　鲁西地区新太古代晚期岩浆岩 Hf、Nd 同位素图解

Fig. 8　Hf and Nd isotopic diagrams of late Neoarchean magmatic rocks in the Luxi area

(a) Crystallization age (t) versus εHf(t) diagram for zircons (data from Wang et al., 2013c; Guo et al., 2014; Gao et al., 2018, 2020; Sun et al., 2019a, 2020; Yu et al., 2021); (b) Crystallization age (t) versus εHf(t) diagram for whole-rocks (data from Jahn et al., 1988; Wang et al., 2013c; Peng et al., 2013; Gao et al., 2018)

11b）。前一组年龄与 C 岩性带内 TTG 片麻岩年龄基本一致，柳杭岩组变质砾岩中砾石成分以 TTG 片麻岩、长英质火山岩等为主（曹国权等，1996），证实了 C 岩性带岩石为副变质岩的物源之一。高 MgO、FeO^T 及后一组年龄峰值表明鲁西地区 B 岩性带内科马提岩、玄武岩也是碎屑岩沉积的重要物源（Wan et al., 2012a; Wang et al., 2014）。这说明鲁西地区 2.55～2.50 Ga 副变质岩为板块俯冲过程中岛弧及古老陆块剥蚀沉积的产物，代表洋壳俯冲过程中的弧后盆地沉积（Wang et al., 2014; Zhang et al., 2025b），华北克拉通东部鞍山–本溪绿岩带内和北缘也发育岛弧–弧后盆地沉积（Dong et al., 2024; Wei et al., 2025）。

4　韧性剪切构造边界

4.1　韧性剪切变形特征

鲁西地区发育一系列北西—北西西走向的韧性剪切带，由北向南包括七星台、南留、雁翎关、新泰、东岭–华村、蒙山、丰阳–梁邱、青邑、白彦等。韧性剪切带具有向北东或南西陡倾的面理和近水平矿物拉伸线理（图 12）。韧性剪切带内广泛发育 a 型褶皱（图 13a）、S-C 组构、旋转碎斑系、书斜构造、云母鱼等不对称构造，指示左行走滑的运动学特征（图 13b—13d, 图 14a—14d）。剪切面理和同构造脉体切割深熔花岗岩脉（图 13e），同构造石英脉与面理平行密集排列（图 13f），斜长石、石英等造岩矿物发生明显塑性拉长变形（图 14e、14f），为挤压应力形成的中—高温（400～600℃）剪切变形带（Wang et al., 2024a）。有限应变测量结果显示，鲁西地区韧性剪切带以压扁变形为特征（张拴宏和周显强，1999; 张书慧等，2025），运动学涡度为 0.79～0.99（Zhang et al., 2022），最大差应力为 75.4～91 MPa（张拴宏和周显强，1999; 王新社等，1999）。同变形矿物 $^{40}Ar/^{39}Ar$ 和同构造脉体锆石 U-Pb 测年显示，韧性剪切带变形时代为 2.58～2.49 Ga（Zhang et al., 2022; Wang et al., 2024a）。

鲁西地区发育与韧性剪切变形同时期的、由洋壳俯冲形成的钙碱性火山岩、高镁安山岩、埃达克岩及赞岐岩等（Peng et al., 2012, 2013; Wang et al., 2013c; Sun et al., 2019a），说明鲁西地区韧性剪切变形带是与洋壳斜向俯冲有关的走滑变形带（Zhang et al., 2022）。构造恢复结果显示，韧性剪切带的初始状态为向北东陡倾的走滑型韧性剪切带。依据左行走滑的运动学特征判断，新太古代晚期胶辽地块与迁怀地块之间的洋壳向南东方向俯冲（Wang et

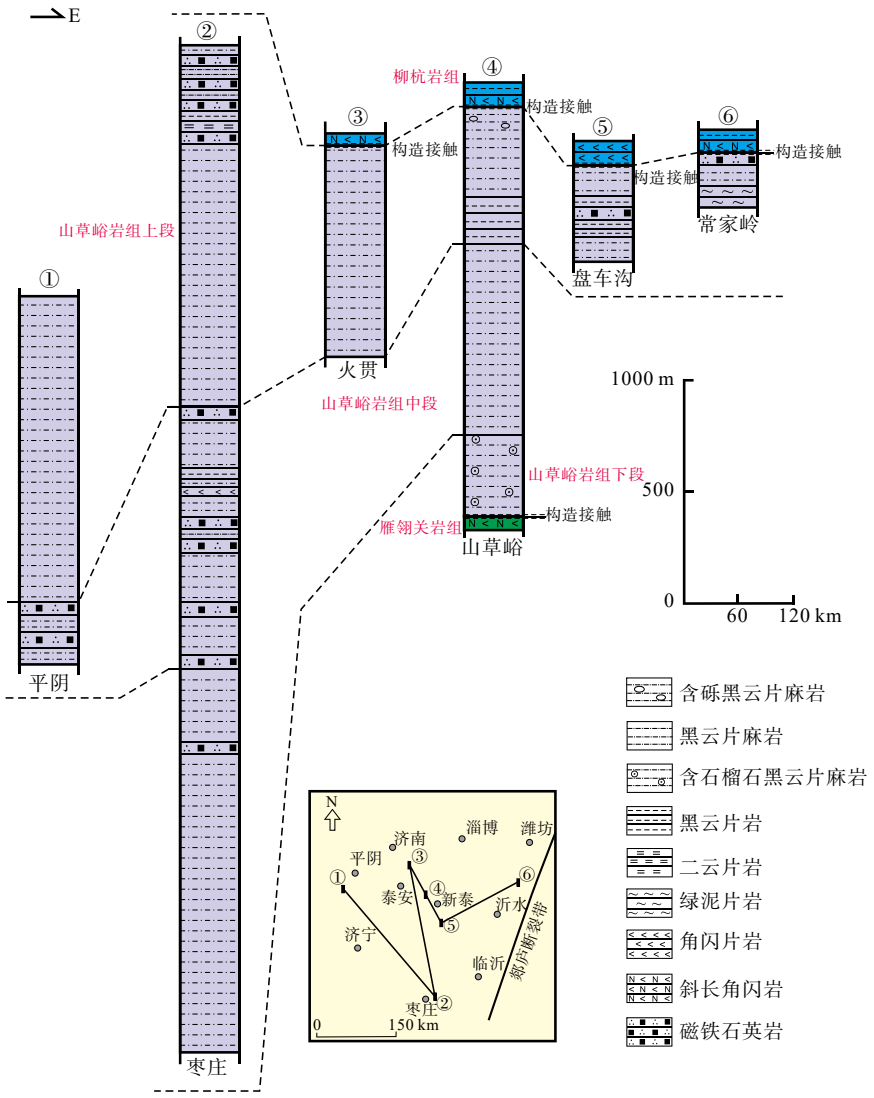


图 9 鲁西地区山草峪岩组地层柱状图

Fig. 9 Stratigraphic column of the Shancaoyu Formation in the Luxi area

al., 2024a)。

部分学者在鲁西地区识别出了早前寒武纪多期变形，包括 2.85～2.80 Ga 伸展变形、2.78～2.71 Ga 北东—南西向挤压缩短变形和 2.58～2.47 Ga 的左行走滑剪切变形(Gao et al., 2019a)，但并未发现新太古代晚期的挤压缩短变形。鲁西地区新太古代晚期多期次变形方面，部分研究认为韧性剪切带发生连续、多期次、但是运动学特征上并无差别的左行走滑(曹国权等, 1996)。但在这一模型中基于相同运动学特征进行变形期次划分依据不足，而且这些变形多数存在于表壳岩中，并未考虑后期岩浆侵入和中新生代脆性断层活动引发的构造变位(Tian and Nutman, 2022)。已有研究表明鲁西地区韧性剪切带以走滑变形为主，但韧性剪切变形岩石电子背散射衍射分析(EBSD)发现石英变形以柱面<a>(550～650℃)和菱面<a>(400～500℃)2 种滑移型式为主，而且矿物的变形行为也表现出 400～500℃ 和 550～650℃ 这 2 个变形温度区间(Wang et al., 2024a)，所以鲁西地区韧性剪切带应经历了早期高温阶段的变形。对早期高温变形特征有 2 种解释：①鲁西地区韧性剪切带表现为长期的走滑剪切并伴随着时代连续的岩浆活动，受控于板块的持续俯冲；②由于后期强烈的走滑剪切变形导致早期的变形特征难以识别，所以变形年龄(2.58～2.49 Ga)应该包括了早期高温变形阶段(Wang et al., 2024a)。

4.2 韧性剪切变形带与构造边界

鲁西地区 C 岩性带、B 岩性带和 A 岩性带的界线与北西向韧性剪切带有一定的空间对应关系(图 15，图 16)，A 岩性带与 B 岩性带之间的界线与南留–蒙山韧性剪切带空间位置基本一致，B 岩性带与 C 岩

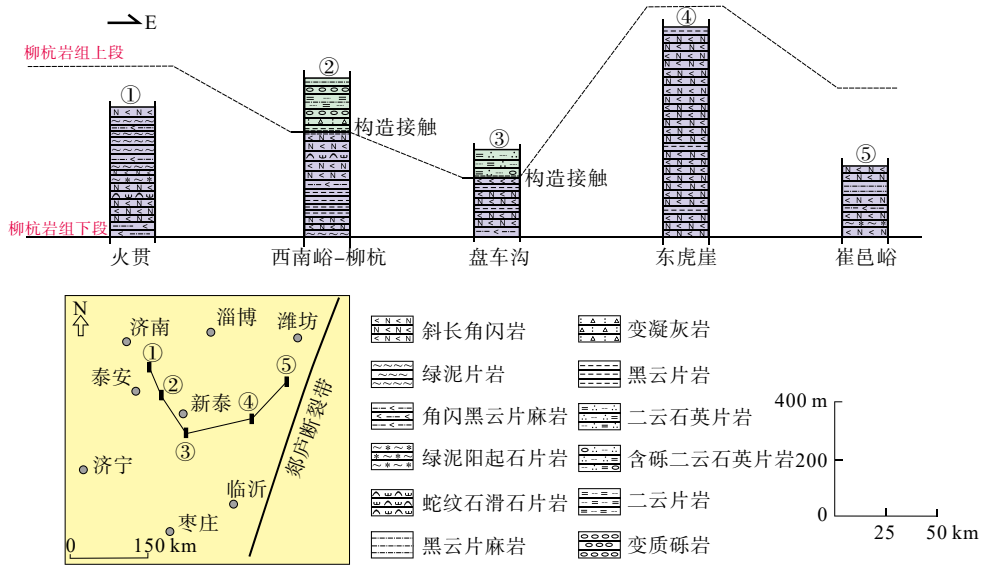
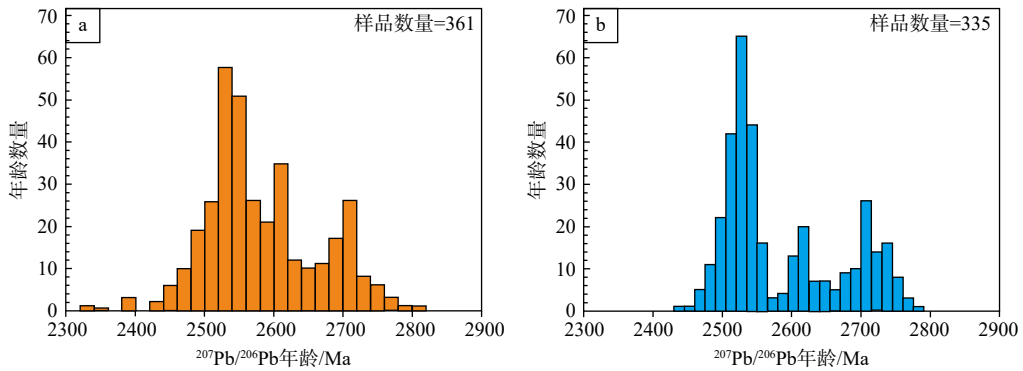


图 10　鲁西地区柳杭岩组地层柱状图

Fig. 10　Stratigraphic column of the Liuhang Formation in the Luxi area



a—新太古代晚期表壳岩系岩石（数据主要来自山草峪岩组和柳行岩组上段的变质沉积岩和长英质变质火山岩）；b—新太古代深成侵入岩

图 11　鲁西地区新太古代晚期表壳岩和侵入岩锆石年龄直方图（Wan et al.，2012a）

Fig. 11　Histogram of apparent $^{207}Pb/^{206}Pb$ ages of late Neoarchean supracrustal rocks and intrusive rocks in the Luxi area (Wan et al., 2012a)

(a) Late Neoarchean supracrustal rocks (data mainly from metamorphic sedimentary rocks and felsic metamorphic volcanic rocks of the Shancaoyu Formation and the upper part of the Liuhang Formation; (b) Neoarchean intrusive rocks

性带之间的岩性界线与七星台–新泰韧性剪切带对应。所以鲁西地区 A、B、C 3 个岩性带代表了 3 个具有不同属性的构造单元，北西向韧性剪切带应该为不同单元之间的构造界线。

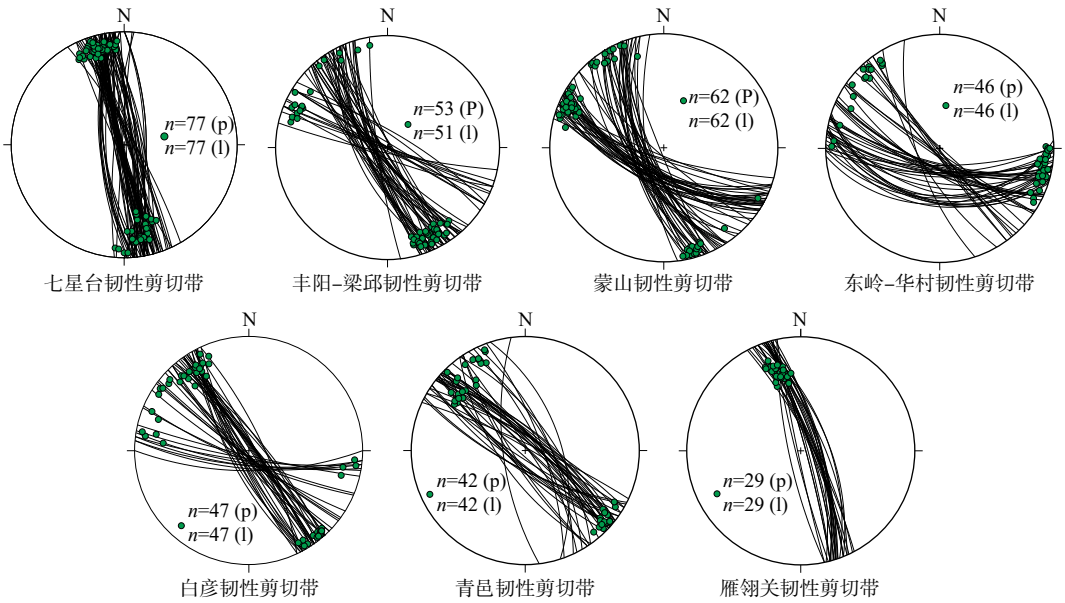
综上可知，鲁西地区发育一系列新太古代晚期增生造山作用标志，包括俯冲洋壳或地幔楔部分熔融形成的岛弧或陆缘弧岩浆岩组合（Sun et al., 2019a; Hu et al., 2019a; Gao et al., 2020; Yang et al., 2020; Yu et al., 2021）、板块斜向汇聚导致的走滑构造变形（Zhang et al., 2022; Wang et al., 2024a）、岛弧沉积盆地（Wang et al., 2014）。因此以往文献中提及的鲁西花岗–绿岩带实际是一条新太古代晚期增生型造山带，即鲁西造山带。

5　讨论

5.1　鲁西造山带构造单元划分及俯冲带位置

5.1.1　构造单元划分

综上可知，鲁西地区 A 岩性带壳源花岗岩形成于俯冲板片回撤过程中软流圈地幔上涌引发的地壳部分熔融（王伟等，2010; Wang et al., 2017b; Yu et al., 2021）；C 岩性带岩浆岩主要来自于俯冲洋壳或被流体、熔体交代的地幔楔又或是下地壳镁铁质岩石的部分熔融（Wang et al., 2009; Sun et al., 2019a; Hu et al., 2019a; Yu et al., 2021）；而 B 岩性带主要由>2.60 Ga 的 TTG 及表壳岩组成（Wan et al., 2010），代表>2.60 Ga 的古老陆



n—构造要素数量; p—面理; l—线理

图 12 鲁西地区韧性剪切带构造要素下半球赤平投影

Fig. 12 Lower-hemisphere stereographic projections of structural elements of the main ductile shear zones in the Luxi area

n—number of structural elements; p—foliation; l—lineation

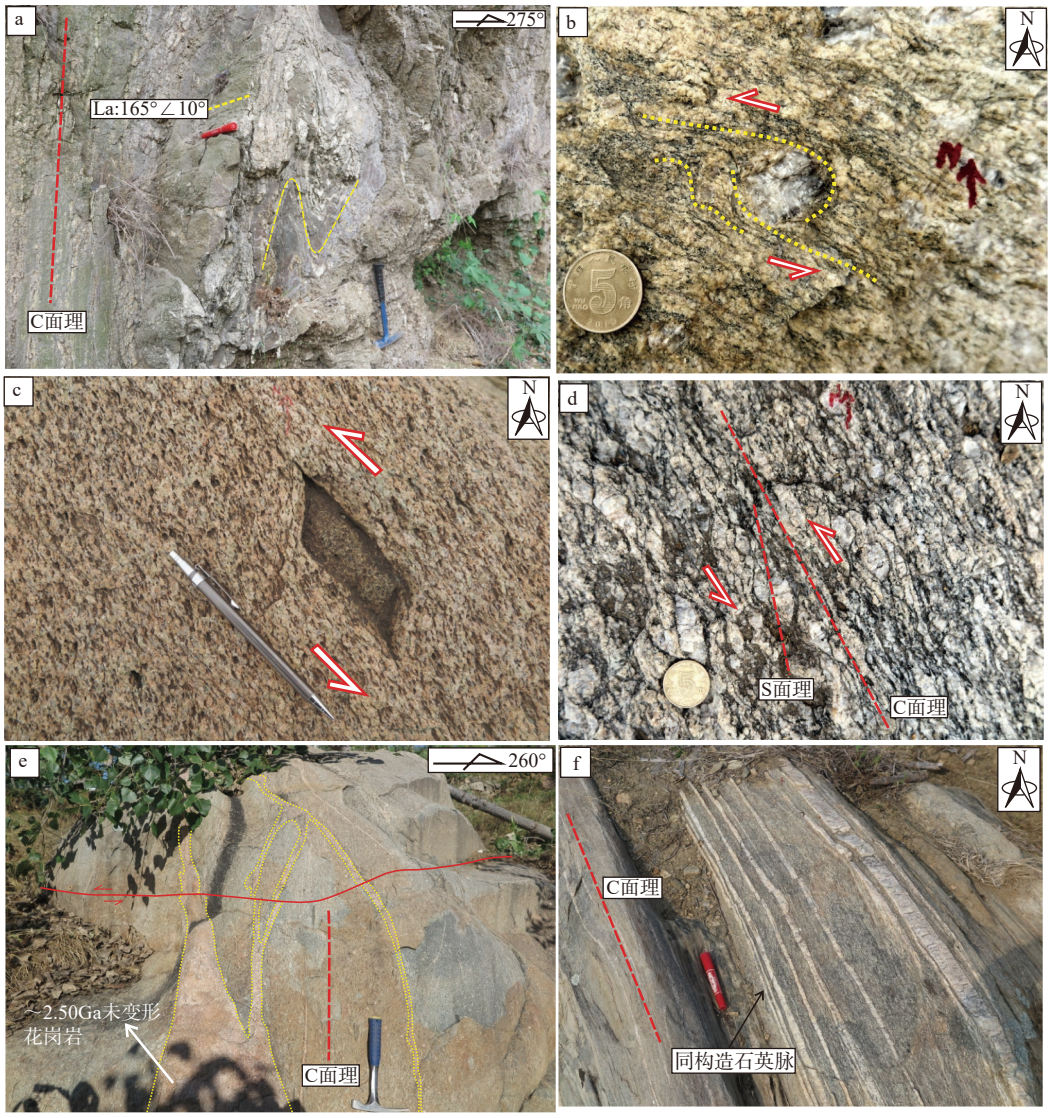
块,物质组成和胶辽地块内部栖霞、莱州地区可以对比(万渝生等,2019)。因此,文章将 Wan et al.(2010)所划分 A、B、C3 个岩性带分别命名为 2.53～2.48 Ga 鲁山–沂水岩浆岩带、2.75～2.60 Ga 七星台–蒙阴地块和 2.56～2.53 Ga 肥城–滕州岩浆弧(图 17)。鉴于七星台–蒙阴地块与胶辽地块之间明显的亲缘性,鲁西造山带应为胶辽地块西南缘新太古代晚期增生型造山带。

5.1.2 俯冲带位置

鲁西地区太古宙基底以绿片岩相–角闪岩相变质为主,并未发现高温高压变质岩(曹国权等,1996)。张增奇等(2012)在新泰地区新太古代晚期二长花岗岩内的暗色包体中发现红宝石,代表 10～40 km 深处地壳岩石(Stern et al., 2013)。但暗色包体可能是在岩浆上升过程中所携带的下地壳岩石,所以红宝石出露的位置并不能代表俯冲带的位置。有研究表明七星台–雁翎关一带的 2.75～2.70 Ga 的基性—超基性岩石代表新太古代早期洋壳(Dong et al., 2021),故推测俯冲带位置在七星台至雁翎关一带。

经分析,由肥城–滕州岩浆弧向鲁山–沂水岩浆岩带,岩浆源区由变质基性岩向变质杂砂岩转变。这种源区的规律变化暗示在洋壳俯冲过程中,靠近海沟主要发育由洋壳或俯冲板片上覆地幔楔部分熔融形成的岩浆岩,向胶辽地块方向则逐步转变为由幔源岩浆底垫导致下地壳部分熔融形成的花岗岩,由早至晚地壳物质的参与程度逐渐增强,据此判断胶辽与迁怀地块之间的洋壳向东俯冲。鲁西造山带内北西向韧性剪切带以左行走滑为主,也指示胶辽与迁怀地块之间洋壳向南东俯冲(Wang et al., 2024a)。七星台–蒙阴地块为一个>2.60 Ga 古老地块,如果主俯冲带位于该地块北东侧的七星台–新泰附近,肥城–滕州陆缘岩浆弧应该位于七星台–蒙阴地块的北东侧,这与现实不符。因此鲁西地区新太古代晚期主俯冲带应位于肥城–滕州岩浆弧的南西侧(图 17),但由于新生代沉积物的严重覆盖,其具体位置难以确定。

值得注意的是,济宁岩群为一套低绿片岩相变质的含铁火山–沉积岩,为海陆过渡性近岸浅海陆架沉积(宋明春等,2011),形成时代约 2.56 Ga(王伟等,2010),而山草峪岩组峰期变质条件可达高角闪岩相(550～570 MPa 和 678～679℃; Wang et al., 2014)。是何种原因造成近于同时代沉积的表壳岩变质程度的差异?通过分析发现,代表弧后盆地沉积的山草峪岩组零散分布于七星台、泰山、枣庄以及韩旺等地,而济宁岩群主要分布在鲁西西部的济宁地区,故推测济宁地区可能为更靠近弧前区域,而山草峪岩组位于弧后的高热流区,从而导致不同的变质程度(图 17)。



La—矿物拉伸线理

a—七星台韧性剪切带中陡倾面理及近水平矿物拉伸线理，枢纽与线理平行的 A 型褶皱；b—东岭–华村韧性剪切带斜长石旋转碎斑指示左行剪切；c—白彦韧性剪切带内斜长角闪岩捕虏体经受变形改造，指示左行剪切；d—蒙山韧性剪切带内 S-C 组构指示左行剪切；e—侵入青邑韧性剪切带未变形的细粒花岗岩脉，测年数据引自 Wang et al.（2024a）；f—丰阳–梁邱韧性剪切带中平行于剪切面理的同构造石英脉

图 13　鲁西地区韧性剪切带宏观变形照片

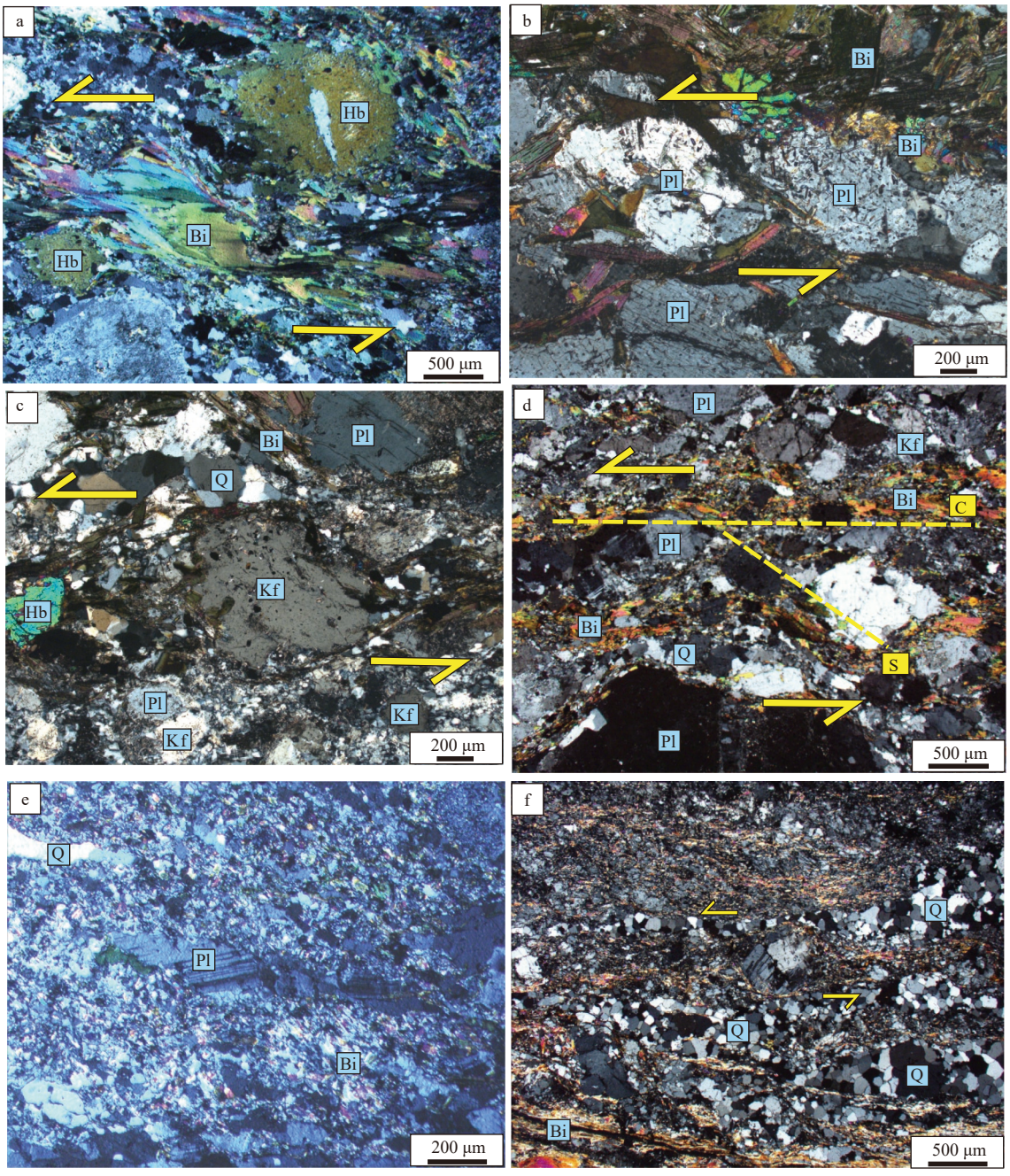
Fig. 13　Photos of macroscopic deformation characteristics of the main ductile shear zones in the Luxi area

(a) Steeply dipping foliation and subhorizontal mineral stretching lineation in the Qixingtai ductile shear zone, with an A-type fold whose hinge is parallel to the lineation; (b) Rotated plagioclase porphyroclasts in the Dongling–Huacun ductile shear zone, indicating sinistral shear; (c) Deformed amphibolite xenolith in the Baiyan ductile shear zone, indicating sinistral shear; (d) S–C fabric in the Mengshan ductile shear zone, indicating sinistral shear; (e) Undeformed fine-grained granite veins intruding the Qingyi ductile shear zone (geochronological data from Wang et al., 2024); (f) Synkinematic quartz veins parallel to the shear foliation in the Fengyang–Liangqiu ductile shear zone

5.2　鲁西增生型造山带构造演化过程

5.2.1　初始洋壳形成阶段（>2.70 Ga）

鲁西地区新太古代早期（>2.7 Ga）科马提岩具有 Nb 亏损的地球化学特征，经历了 2%～6% 的古老地壳的混染和橄榄石的分离结晶作用（Polat et al., 2006）。残存的橄榄石温度计显示其喷发温度约 1300℃（Cheng and Kusky, 2007），指示新太古代早期鲁西地区以地幔柱为主导构造体制（Yu et al., 2022; Zuo et al., 2025）。Dong et al.（2021）认为鲁西地区>2.70 Ga 的基性—超基性火山岩代表了新太古代早期的初始洋壳。所以，在新太古代早期，镁铁质—超镁铁质初始洋壳从地幔中分异出来，鲁西地区经



Hb—角闪石；Bi—黑云母；Pl—斜长石；Q—石英；Kf—钾长石

a—白彦韧性剪切带内云母鱼、角闪石旋转碎斑指示左行剪切；b—蒙山韧性剪切带斜长石书斜构造；c—丰阳–梁邱韧性剪切带斜长石旋转碎斑，指示左行剪切；d—七星台韧性剪切带中 S-C 组构指示左行剪切，C 面理由石英多晶条带和黑云母定向排列构成；e—丰阳–梁邱韧性剪切带内斜长石拉长变形；f—七星台韧性剪切带内多晶石英条带，长石旋转碎斑指示左行剪切

图 14 鲁西地区韧性剪切带显微变形照片

Fig. 14 Microphotographs of the main ductile shear zones in the Luxi area

(a) Mica fish and rotated hornblende porphyroclasts in the Baiyan ductile shear zone, indicating sinistral shear; (b) Plagioclase domino structure in the Mengshan ductile shear zone, indicating sinistral strike-slip shear; (c) Rotated plagioclase porphyroclasts in the Fengyang–Liangqiu ductile shear zone, indicating sinistral shear; (d) S-C fabric in the Qixingtai ductile shear zone, with C-foliation defined by polycrystalline quartz ribbons and oriented biotite, indicating sinistral shear; (e) Elongated plagioclase in the Fengyang–Liangqiu ductile shear zone; (f) Polycrystalline quartz ribbons and rotated plagioclase porphyroclasts in the Qixingtai ductile shear zone, indicating sinistral shear

Hb—hornblende; Bi—biotite; Pl—plagioclase; Q—quartz; Kf—K-feldspar

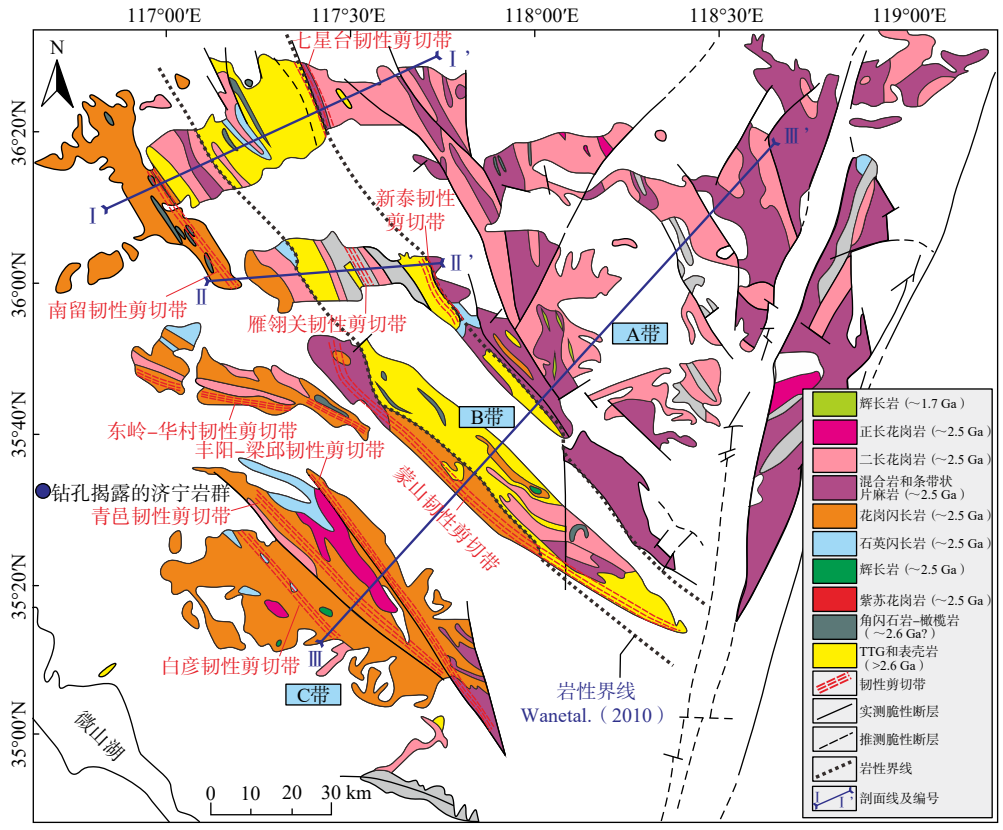


图 15　鲁西地区岩性分带界线与韧性剪切带的空间对应关系

Fig. 15　The spatial correspondence between lithologic zonation boundaries and ductile shear zones in the Luxi area

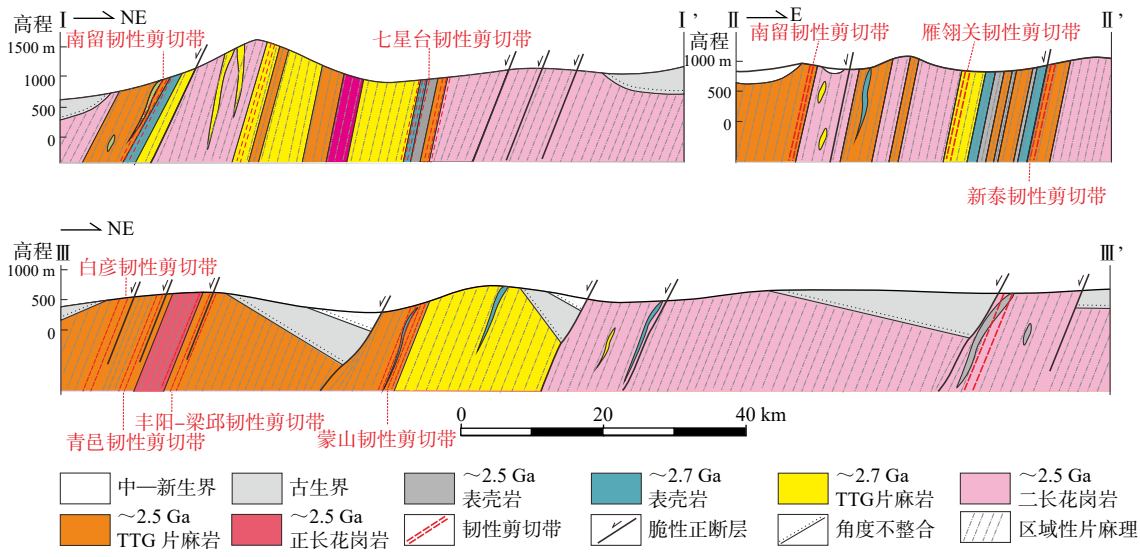


图 16　鲁西地区构造–岩性剖面图（剖面位置见图 15）

Fig. 16　Structural–lithological cross-sections of the Luxi area

历了地幔柱主导的初始洋壳形成阶段，以雁翎关岩组和柳杭岩组下段科马提岩和玄武岩为代表，这一阶段为后续洋壳俯冲提供了先决条件（图 18a）。

5.2.2　初始洋壳俯冲阶段（2.70～2.60 Ga）

目前，对于鲁西地区 2.60 Ga 构造–岩浆事件的背景尚存在不同认识。一种观点认为 2.60 Ga 的富钠灰色片麻岩是由 2.75～2.60 Ga 英云闪长岩和斜长角闪岩陆壳部分熔融形成，形成于地幔柱或地幔翻转背景下软流圈上涌的伸展构造体制，部分熔融过程中有海水和大气降水流体参与（Wang et al., 2016;

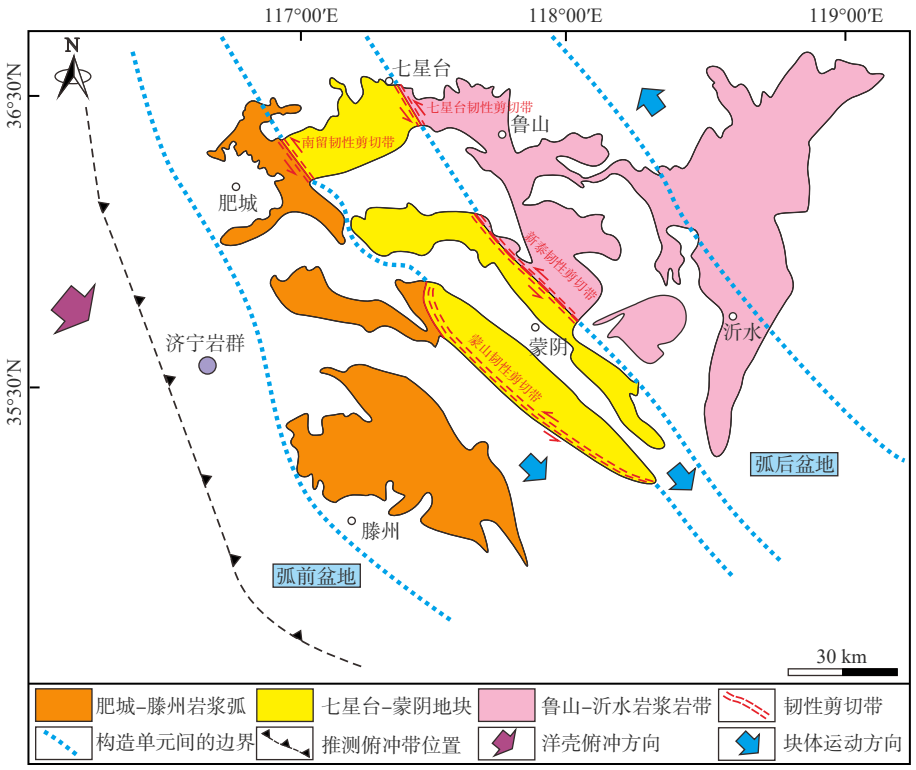


图 17 鲁西增生型造山带构造单元划分及块体拼贴方式示意图

Fig. 17 Schematic diagram showing the tectonic subdivision and terrane amalgamation of the Luxi accretionary orogenic belt

王伟等, 2016; Ren et al., 2016; Yakymchuk et al., 2019), 部分岩石源区接近同时期的亏损地幔(Wan et al., 2014b)。另一种观点认为 2.62 Ga 的英云闪长岩、2.59 Ga 的花岗闪长质片麻岩及 2.61～2.58 Ga 二长花岗质片麻岩的源区分别为俯冲洋壳、拆离的下地壳镁铁质岩和硬砂岩的部分熔融, 指示在 2.70～2.60 Ga 鲁西地区存在板块俯冲过程(Hu et al., 2019b)。基于地幔柱构造体制下初始洋壳的形成阶段(>2.7 Ga), 2.70～2.60 Ga 期间鲁西地区地幔温度可能有所降低, 局部初始洋壳开始发生俯冲(图 18b), 代表了地幔柱构造体制与板块构造体制的过渡阶段(Wang et al., 2024b)。

5.2.3 洋壳俯冲及弧–陆碰撞阶段(2.58～2.49 Ga)

新太古代晚期(2.58～2.49 Ga), 胶辽地块与迁怀地块之间以绿岩带代表的初始洋壳在重力的作用下开始下沉、俯冲(Guo et al., 2024; Liu et al., 2024a, 2024b), 板块构造成为鲁西地区的主导构造体制(图 18c)。洋壳俯冲过程中, 被流体或熔体交代的地幔楔及下地壳的部分熔融形成岛弧拉斑玄武岩、高镁安山岩、玻安岩、赞岐岩和埃达克岩等岩浆岩组合(Peng et al., 2012; Sun et al., 2019b; Yu et al., 2021), 同时在弧后盆地沉积了一套火山–碎屑岩(Wang et al., 2014)。约 2.54 Ga 俯冲洋壳发生板片回撤, 鲁西造山带处于伸展构造体制, 软流圈地幔上涌导致地壳的部分熔融, 形成大规模壳源花岗岩, 早期岩石发生强烈的混合岩化(Yu et al., 2019, 2021)。鲁西造山带内韧性剪切带在洋壳长期俯冲过程中持续变形。新太古代侵入体北西向拉长透镜状的几何学形态、韧性剪切变形与岩浆活动之间密切的时间关系说明, 韧性变形为同岩浆期变形, 对于岩浆的运移和侵位起重要的控制作用。这一阶段也是鲁西增生型造山带重要的地壳增生和活化阶段(Wan et al., 2010)。

5.2.4 构造寂静期(2.49～2.34 Ga)

新太古代晚期胶辽地块与迁怀地块拼合之后, 古元古代早期, 鲁西造山带并未经历强烈的构造–岩浆事件。华北克拉通也已形成了统一的克拉通基底并处于构造寂静期(图 18d), 大陆地壳厚度较大、刚性程度较高, 华北克拉通由始板块构造向早期板块构造体制过渡(翟明国等, 2020)。

5.2.5 陆内伸展演化阶段(2.34～1.85 Ga)

华北克拉通发育新太古代晚期(约 2.50 Ga)和古元古代晚期(1.95～1.85 Ga)2 期重要的构造–变质事件。前者代表华北克拉通新太古代晚期微陆块拼合碰撞的克拉通化过程, 后者代表古元古代晚期

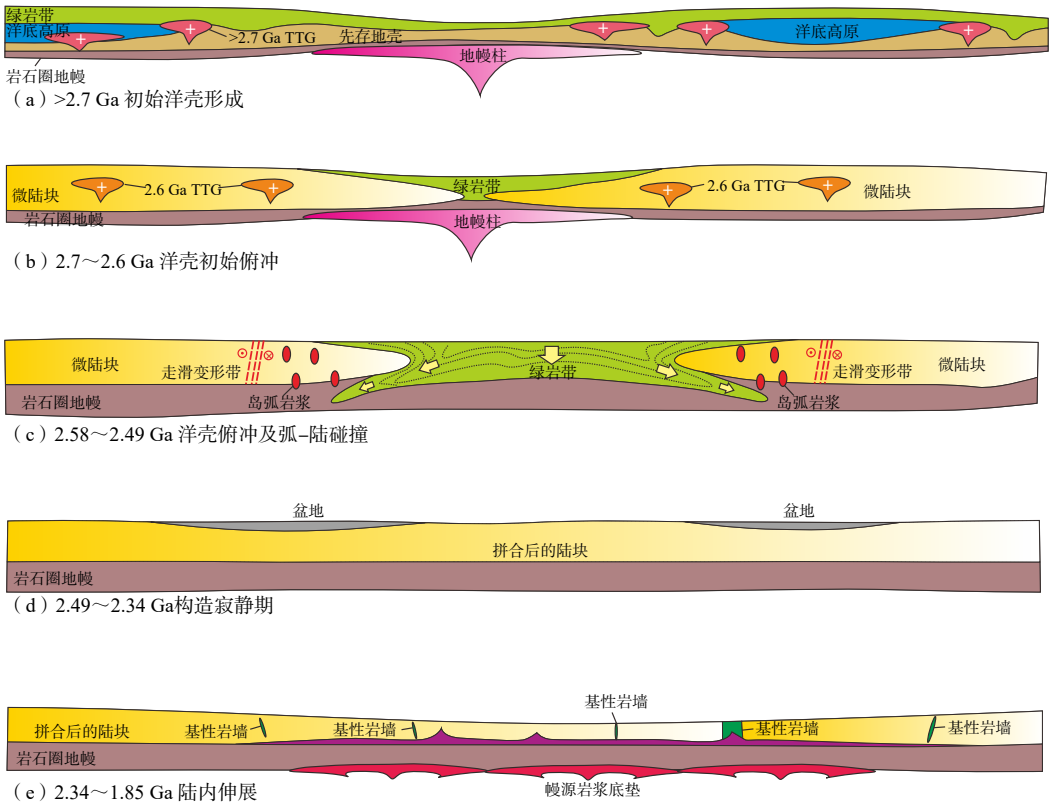


图 18　鲁西增生型造山带构造演化示意图（据翟明国等，2020 修改）

Fig. 18　Tectonic evolution model of the Luxi accretionary orogenic belt (modified after Zhai et al., 2020)

Cartoon showing tectonic evolution model of the Luxi accretionary orogenic belt (modified after Zhai et al., 2020)

(a) Formation of the initial oceanic crust (>2.70 Ga); (b) Initial subduction of the oceanic crust (2.7-2.6 Ga); (c) Oceanic crust subduction and arc-continent collision (2.58-2.49 Ga); (d) Tectonic quiescence period (2.49-2.34 Ga); (e) Intracontinental extension stage (2.34-1.85 Ga)

陆内裂解–俯冲–碰撞造山事件，形成晋豫、胶辽和丰镇 3 条构造活动带（Zhai and Santosh, 2011; Zhao and Zhai, 2013）。变质锆石定年显示，鲁西地区早前寒武纪最晚的构造–变质事件为古元古代早期（2.48～2.45 Ga），尚未发现与古元古代造山作用对应的 1.95～1.85 Ga 的变质事件（Dong et al., 2017），鲁西地区是否存在古元古代的构造事件尚不清楚。近年来，部分学者在鲁西造山带内识别出 2.34 Ga、2.09 Ga 和 1.84 Ga 镁铁质岩墙，代表陆–陆碰撞后或陆内裂谷等伸展背景（Hou et al., 2006; Wang et al., 2007; Yang et al., 2019; Zhang et al., 2023）。Wang et al.（2024a）也在鲁西地区韧性剪切带内获得了 3 个黑云母古元古代 $^{40}Ar/^{39}Ar$ 年龄，分别为 2328±5 Ma、1916±8 Ma 和 1856±7 Ma，因此可以确定鲁西造山带在古元古代受陆内伸展构造背景下幔源岩浆底垫影响。这一伸展构造事件与华北克拉通古元古代期间的裂解、俯冲、碰撞有关（Zhai et al., 2005; Yang et al., 2021; Mu et al., 2022; Kang et al., 2024; Ouyang et al., 2024），同时也说明新太古代期间华北克拉通就已完成了以洋壳俯冲、弧–陆碰撞方式的克拉通化，于古元古代期间转为陆内构造演化阶段（图 18e）。

5.3　新太古代晚期胶辽地块周缘地壳增生事件

鲁西造山带位于胶辽地块西缘，是胶辽地块与迁怀地块之间拼合带（Zhai and Santosh, 2011）。新太古代晚期，胶辽地块与迁怀地块之间的洋壳发生俯冲，肥城–滕州岩浆弧与七星台–蒙阴地块通过七星台–新泰韧性剪切带斜向拼贴。韧性剪切带左行走滑运动学特征显示块体向南东汇聚的极性特征（图 19），代表弧–陆碰撞的侧向地壳增生；同时，鲁西地区新太古代晚期岩浆岩由俯冲板片或亏损地幔部分熔融形成（Wang et al., 2009; Peng et al., 2012; Sun et al., 2019a; Hu et al., 2019a），代表地壳的垂向增生。在冀东地区，新太古代晚期岩浆岩岩石类型多样，且形成时代集中在 2.55～2.45 Ga 这一短暂的时间内（Geng et al., 2006）。岩浆源区主要以年轻组分及富集地幔的部分熔融（Yang et al., 2008; Zhang et al., 2024），表明胶辽地块西缘新太古代晚期存在强烈的地壳增生事件（Zhang et al., 2024）。Yang et al.（2016a,

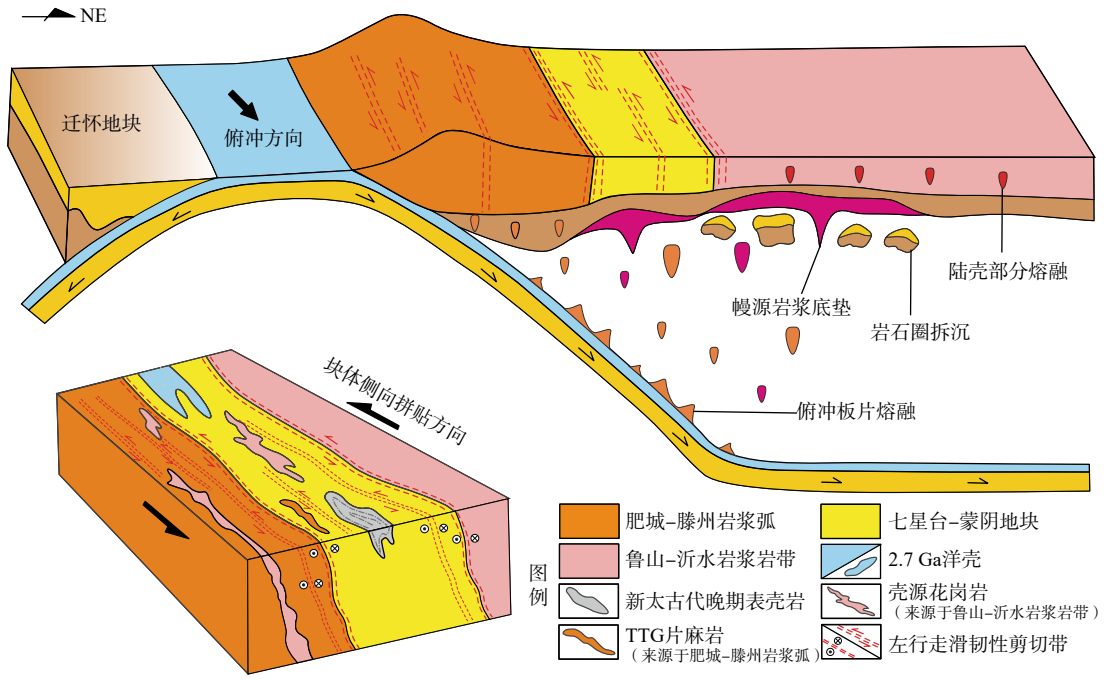


图 19 胶辽地块西缘鲁西地区洋壳俯冲以及块体拼合示意图

Fig. 19 Tectonic model showing the subduction of ocean crust and terrane amalgamation in the Luxi area on the western margin of the Jiaoliao Block

2016b)也认为胶辽地块西缘发育 2.59～2.54 Ga 弧岩浆作用,并伴随着高级变质作用。

胶辽地块北缘的岩浆作用存在 5 个明显的峰值,主要峰值年龄为 2522±5 Ma,代表了胶辽地块北缘新太古代晚期陆壳增生事件;其余 4 个峰值分别为 2982±12 Ma、3138±12 Ma、3338±8 Ma 和 3809±6 Ma,代表始太古代—中太古代期间的地壳增生(Yang and Santosh, 2017; Li et al., 2021)。也有研究表明胶辽地块北缘辽北地体在 2530 Ma 之后增生至华北克拉通北缘,标志陆块的最终拼合(Wang et al., 2017c)。辽北地体西南缘发育新太古代晚期的洋内弧,在太古代晚期拼贴至东部陆块上(Wang et al., 2015, 2016b)。吉南地体在约 2.55 Ga 也发生以板块构造体制为主导的地壳增生活化(Wu et al., 2021; Liu et al., 2022; Liu et al., 2025)。

胶辽地块东缘沂水地区发育 2.56～2.53 Ga 的岛弧或陆缘弧岩浆作用。岩浆来源于俯冲大洋板块的部分熔融(Peng et al., 2012; Li et al., 2016),并伴随着古老陆壳的循环(Wu et al., 2013),为胶辽地块西缘和南缘的迁怀地块和徐淮地块在新太古代晚期—古元古代初期同时向胶辽地块汇聚,形成的巨型俯冲–碰撞增生体系(Santosh et al., 2016; Li et al., 2016)。胶东地区在新太古代晚期(约 2.52 Ga)也发生强烈的地壳增生事件(Yang et al., 2017; He et al., 2021; Chen et al., 2025)。因此,新太古代晚期华北克拉通东部克拉通化过程是以胶辽地块为中心(图 20),周边微陆块通过洋壳俯冲及弧–陆或陆–陆碰撞的形式与胶辽地块拼贴。

5.4 新太古代晚期板块热俯冲引发地壳增生事件

2.60～2.50 Ga 期间华北克拉通东部发育广泛的板块俯冲过程,形成一系列板块俯冲地质记录,包括鞍山、冀北—冀东、辽西、辽南、吉南、胶北等地区发育的新太古代晚期板块俯冲岛弧火山岩和壳源花岗岩(Wan et al., 2015; Guo et al., 2017a, 2017b, 2022, 2025; Wang et al., 2017a; Gao et al., 2020; Fu et al., 2021),密云、沂水和赞皇等地发育的约 2.50 Ga 蛇绿岩残片(Kusky and Zhai, 2012; Santosh et al., 2016, 2020),与板块汇聚有关的逆冲推覆构造、走滑韧性剪切带及构造混杂岩(Wang et al., 2013a; Zhong et al., 2021; Zhang et al., 2022; Wang et al., 2024a)。早期板块俯冲的形式和演化受控于板块边缘的热状态及冷却速率(Palin et al., 2020; Zheng and Zhao, 2020)。华北克拉通早前寒武纪的地温梯度明显高于显生宙造山带(Sun et al., 2019b; 翟明国等, 2020; 刘树文等, 2021; Li et al., 2023),并且从中太古代至新太古代晚期地幔温度逐渐降低(Sun et al., 2021),所以华北克拉通在新太古代晚期以板块构造体制为主导。新太古代晚期板块俯冲及弧–陆碰撞过程与现代板块构造

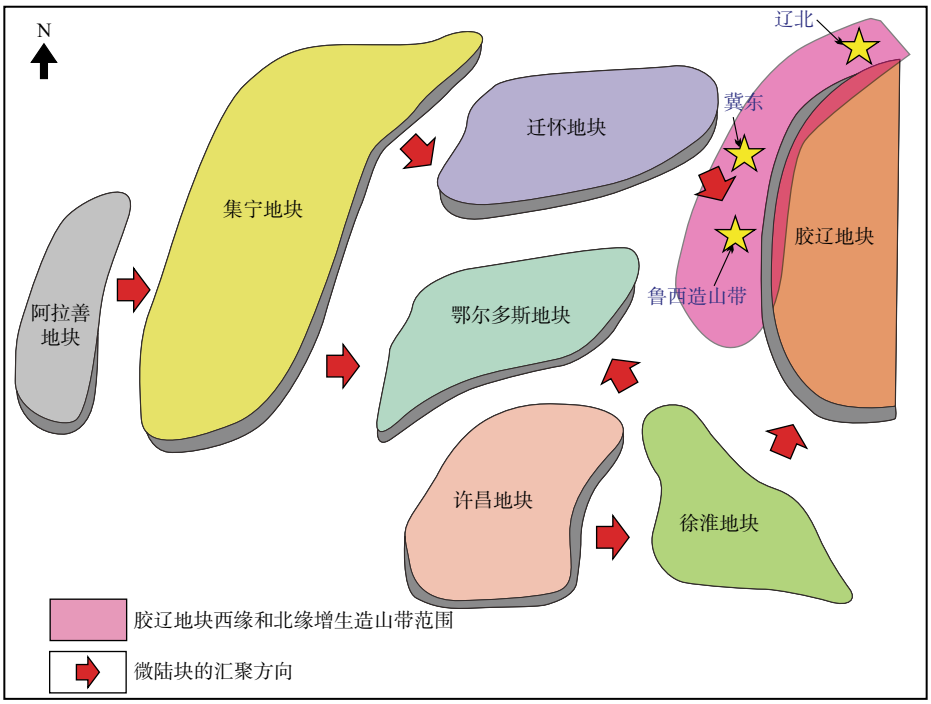


图 20　华北克拉通微陆块拼合方向示意图（据 Zhai and Santosh，2011 修改）

Fig. 20　Schematic diagram showing the convergence direction of micro-blocks in the North China Craton (modified after Zhai and Santosh, 2011)

体制有类似的表现形式，但在俯冲深度以及俯冲频率方面还是存在明显差异，表现为规模小、俯冲角度大，俯冲板片回转和断离深度明显低于现代板块构造体制的热俯冲（刘树文等，2021；Sun et al., 2021, 2025；Wang et al., 2024c）。也有研究认为新太古代末鲁西地区缺少大型的逆冲变形及高级变质作用，与中亚造山带、阿尔卑斯造山带、喜马拉雅造山带、秦岭–大别山造山带等明显不同，因此并不存在俯冲–碰撞造山过程（张书慧等，2025）。鲁西地区缺少上述标志应归因于太古宙时期板块边缘相对较高的地热梯度，导致岩石圈刚性程度下降，板块之间以软碰撞为特点，有些学者就用类似的模型解释江南造山带存在 980～950 Ma 沟弧体系但缺乏中—高级变质作用这一现象（Shu et al., 2021）。虽然板块俯冲的驱动机制和俯冲样式不同于显生宙造山带，但华北克拉通东部在新太古代晚期已存在岩石圈板块大规模的水平移动，新太古代晚期板块构造体制在地幔冷却、岩石圈刚性程度增加和地壳增生等方面发挥了重要作用，并最终形成稳定的克拉通基底。

6　结论

（1）鲁西地区完整保存了新太古代晚期多尺度构造–岩浆记录：岛弧和陆缘弧岩浆岩、碰撞后改造、弧后盆地沉积和板块斜向汇聚的走滑剪切变形。其限定了鲁西花岗–绿岩带为新太古代晚期的增生型造山带，代表胶辽地块西缘的活动大陆边缘。

（2）鲁西增生型造山带可划分为鲁山–沂水岩浆岩带、七星台–蒙阴地块和肥城–滕州岩浆弧 3 个构造单元，各单元之间以高应变韧性剪切带为界，反映俯冲带前缘的构造叠置过程。

（3）鲁西地区新太古代晚期地壳增生方式包括弧–陆斜向碰撞的水平增生和幔源岩浆底垫的垂向增生，揭示了早期板块构造体制下热俯冲–幕式增生的独特动力学模式。

作者贡献声明： 王东明、胡健民负责论文构思、数据分析、研究方法和论文写作；赵远方、闫纪元、公王斌参与数据分析和技术手段的实践应用和绘图；张志刚参与数据分析、研究方法和修改。所有作者均阅读并同意稿件的提交和发表。

Author's Contributions: WANG Dongming and HU Jianmin conceived the study, performed data analysis, designed the research methodology, and drafted the manuscript; ZHAO Yuanfang, YAN Jiyuan and GONG Wangbin participated in data analysis, practical application

of technical approaches, and figure generation; ZHANG Zhigang was involved in data analysis, refinement of the research methodology, and manuscript revision. All authors have read and approved the submission and publication of the manuscript.

利益冲突声明：本文所有作者声明本研究无任何利益冲突。

Conflict of Interests： All authors declare no conflict of interests.

References

ALTHERR R, HOLL A, HEGNER E, et al., 2000. High-potassium, calc-alkaline I-type plutonism in the European Variscides: northern Vosges (France) and northern Schwarzwald (Germany)[J]. Lithos, 50(1-3): 51-73.

BAO H, LIU S W, WAN Y S, et al., 2022. Neoarchean granitoids and tectonic regime of lateral growth in northeastern North China Craton[J]. Gondwana Research, 107: 176-200.

BROWN M, JOHNSON T, GARDINER N J, 2020. Plate tectonics and the Archean Earth[J]. Annual Review of Earth and Planetary Sciences, 48: 291-320.

CAO G Q, 1996. Early Precambrian geology of western Shandong[M]. Beijing: Geological Publishing House: 1-210. (in Chinese)

CAWOOD P A, KRÖNER A, COLLINS W J, et al., 2009. Accretionary orogens through Earth history[J]. Geological Society, London, Special Publications, 318(1): 1-36.

CAWOOD P A, HAWKESWORTH C J, DHUIME B, 2013. The continental record and the generation of continental crust[J]. GSA Bulletin, 125(1-2): 14-32.

CAWOOD P A, HAWKESWORTH C J, PISAREVSKY S A, et al., 2018. Geological archive of the onset of plate tectonics[J]. Philosophical Transactions of the Royal Society A: Mathematical, Physical and Engineering Sciences, 376(2132): 20170405.

CHEN Y P, KONG F M, LI X P, et al., 2025. Multi-mineral dating of Archean granitoids of the Jiaobei Terrane: decoding multiple tectonothermal events in the eastern North China Craton[J]. Precambrian Research, 427: 107864.

CHENG S H, KUSKY T, 2007. Komatiites from west Shandong, North China craton: implications for plume tectonics[J]. Gondwana Research, 12(1-2): 77-83.

CONDIE K C, 1981. Archean greenstone belts[M]. Amsterdam: Elsevier Scientific Publishing Company: 1-425.

CONDIE K C, 2005. Earth as an evolving planetary system[M]. Amsterdam: Elsevier Academic Press: 1-447.

CONDIE K C, 2007. Accretionary orogens in space and time[M]//HATCHER JR R D, CARLSON M P, MCBRIDE J H, et al. 4-D framework of continental crust. Boulder: Geological Society of America: 145-158.

DEWEY J F, KISEEVA E S, PEARCE J A, et al., 2021. Precambrian tectonic evolution of Earth: an outline[J]. South African Journal of Geology, 124(1): 141-162.

DIWU C, SUN Y, SI B W, et al., 2024. Archean continental crustal growth and reworking of the North China Craton: constraints from zircon U-Pb age and Hf isotopic composition[J]. Earth-Science Reviews, 248: 104624.

DONG C Y, XIE H Q, KRÖNER A, et al., 2017. The complexities of zircon crystllazition and overprinting during metamorphism and anatexis: an example from the late Archean TTG terrane of western Shandong Province, China[J]. Precambrian Research, 300: 181-200.

DONG C Y, BAI W Q, XIE H Q, et al. , 2021. Early Neoarchean oceanic crust in the North China Craton: evidence from geology, geochemistry and geochronology of greenstone belts in western Shandong[J]. Lithos, 380-381: 105888.

DONG Z Y, DENG H, KUSKY T, et al., 2024. Growth of the Central Orogenic Belt, North China Craton through accretion of different Neoarchean arc terranes: perspective from the Linshan complex[J]. Precambrian Research, 412: 107555.

DU L L, ZHUANG Y X, YANG C H, et al., 2003. Characters of zircons in the Mengjiatun Formation in Xintai of Shandong and their chronological significance[J]. Acta Geologica Sinica, 77(3): 359-366. (in Chinese with English abstract)

DU L L, ZHUANG Y X, YANG C H, et al., 2005. SHRIMP U-Pb zircon chronology of fine-grained amphibolite in the Mengjiatun area, western Shandong[J]. Acta Geoscientica Sinica, 26(5): 429-434. (in Chinese with English abstract)

FU J H, LIU S W, SUN G Z, et al., 2021. Two contrasting Neoarchean metavolcanic rock suites in eastern Hebei and their geodynamic implications for the northern North China Craton[J]. Gondwana Research, 95: 45-71.

GAO L, LIU S W, SUN G Z, et al., 2018. Petrogenesis of late Neoarchean high-K granitoids in the Western Shandong terrane, North China Craton, and their implications for crust-mantle interactions[J]. Precambrian Research, 315: 138-161.

GAO L, LIU S W, ZHANG B, et al., 2019a. A Ca. 2.8-Ga plume-induced intraoceanic arc system in the eastern North China craton[J]. Tectonics, 38(5): 1694-1717.

GAO L, LIU S W, SUN G Z, et al., 2019b. Neoarchean crust-mantle interactions in the Yishui Terrane, south-eastern margin of the North China Craton: constraints from geochemistry and zircon U-Pb-Hf isotopes of metavolcanic rocks and high-K granitoids[J]. Gondwana Research, 65: 97-124.

GAO L, LIU S W, WANG M J, et al., 2020. Late Neoarchean volcanic rocks in the southern Liaoning Terrane and their tectonic implications for the formation of the eastern North China Craton[J]. Geoscience Frontiers, 11(3): 1053-1068.

GAO M, ZHANG Z J, CHENG Q M, et al., 2021. Zircon U-Pb and Lu-Hf isotopes of Huai'an complex granites, North China Craton: implications for crustal growth, reworking and tectonic evolution[J]. Gondwana Research, 90: 118-134.

GENG Y S, LIU F L, YANG C H, 2006. Magmatic event at the end of the Archean in eastern Hebei province and its geological implication[J]. Acta Geologica Sinica (English Edition), 80(6): 819-833.

GHOSH S, D'SOUZA J, GOUD B R, et al., 2022. A review of the Precam-

brian tectonic evolution of the Aravalli Craton, northwestern India: structural, metamorphic and geochronological perspectives from the basement complexes and supracrustal sequences[J]. Earth-Science Reviews, 232: 104098.

GUO B R, LIU S W, SANTOSH M, et al., 2017a. Neoarchean arc magmatism and crustal growth in the north-eastern North China Craton: evidence from granitoid gneisses in the Southern Jilin Province[J]. Precambrian Research, 303: 30-53.

GUO M J, ZHANG J, QIAN J H, et al. , 2024. Ultrahigh-temperature metamorphism of the felsic granulites in the eastern North China Craton and their implications on the Neoarchean tectonic regime[J]. Lithos, 468-469: 107516.

GUO P, SANTOSH M, LI S R, et al., 2014. Crustal evolution in the central part of eastern NCC: zircon U-Pb ages from multiple magmatic pulses in the Luxi area and implications for gold mineralization[J]. Ore Geology Reviews, 60: 126-145.

GUO R R, LIU S W, GONG E P, et al., 2017b. Arc-generated metavolcanic rocks in the Anshan-Benxi greenstone belt, North China Craton: constraints from geochemistry and zircon U-Pb-Hf isotopic systematics[J]. Precambrian Research, 303: 228-250.

GUO R R, LI Z H, LIU S W, et al., 2022. Late Neoarchean geodynamic regime of the northeastern North China Craton: constraints from metamorphosed volcanic rocks of the Anshan-Benxi greenstone belt[J]. Precambrian Research, 371: 106583.

GUO R R, XIAO Y, WEI C M, et al., 2025. New geochronological evidences and diverse arc-related *meta*-volcanic rock suits from the Northern Liaoning terrane, North China Craton[J]. Precambrian Research, 422: 107755.

HE X, WANG W, SANTOSH M, et al., 2021. Late Neoarchean crustal growth under paired continental arc-back arc system in the North China Craton[J]. Geoscience Frontiers, 12(3): 101120.

HOU G T, LIU Y L, LI J H, 2006. Evidence for ～1.8 Ga extension of the Eastern Block of the North China Craton from SHRIMP U–Pb dating of mafic dyke swarms in Shandong Province[J]. Journal of Asian Earth Sciences, 27(4): 392-401.

HU Y L, LIU S W, GAO L, et al. , 2019b. Diverse middle Neoarchean granitoids and the delamination of thickened crust in the Western Shandong Terrane, North China Craton[J]. Lithos, 348-349: 105178.

HU Y L, LIU S W, SUN G Z, et al., 2019a. Petrogenesis of the Neoarchean granitoids and crustal oxidation states in the Western Shandong Province, North China Craton[J]. Precambrian Research, 334: 105446.

JAHN B M, AUVRAY B, SHEN Q H, et al., 1988. Archean crustal evolution in China: the Taishan complex, and evidence for juvenile crustal addition from long-term depleted mantle[J]. Precambrian Research, 38(4): 381-403.

KANG J L, PENG P, WANG H C, et al., 2024. Continental subduction in Paleoproterozoic: insights from ～ 1.9 Ga nepheline syenite in the North China craton[J]. Precambrian Research, 404: 107346.

KEMP A I S, HAWKESWORTH C J, COLLINS W J, et al., 2009. Isotopic evidence for rapid continental growth in an extensional accretionary orogen: the Tasmanides, eastern Australia[J]. Earth and Planetary Science Letters, 284(3-4): 455-466.

KORSCH R J, KOSITCIN N, CHAMPION D C, 2011. Australian island arcs through time: geodynamic implications for the Archean and Proterozoic[J]. Gondwana Research, 19(3): 716-734.

KUSKY T M, ZHAI M G, 2012. The neoarchean ophiolite in the North China craton: early Precambrian plate tectonics and scientific debate[J]. Journal of Earth Science, 23(3): 277-284.

KUSKY T M, WINDLEY B F, POLAT A, 2018. Geological evidence for the operation of plate tectonics throughout the Archean: records from Archean paleo-plate boundaries[J]. Journal of Earth Science, 29(6): 1291-1303.

LAURENT O, DOUCELANCE R, MARTIN H, et al., 2013. Differentiation of the late-Archaean sanukitoid series and some implications for crustal growth: insights from geochemical modelling on the Bulai pluton, Central Limpopo Belt, South Africa[J]. Precambrian Research, 227: 186-203.

LI S S, SANTOSH M, CEN K, et al., 2016. Neoarchean convergent margin tectonics associated with microblock amalgamation in the North China Craton: evidence from the Yishui Complex[J]. Gondwana Research, 38: 113-131.

LI Z, WEI C J, CHEN B, et al., 2021. U–Pb–Hf–O–Nd isotopic and geochemical constraints on the origin of Archean TTG gneisses from the North China Craton: implications for crustal growth[J]. Precambrian Research, 354: 106078.

LI Z S, SHAN X L, LIU J, et al., 2023. Late Neoarchean TTG and monzogranite in the northeastern North China Craton: implications for partial melting of a thickened lower crust[J]. Gondwana Research, 115: 201-223.

LIOU P, GUO J H, PENG P, et al., 2022. Crustal growth of the North China Craton at ca. 2.5 Ga[J]. Science Bulletin, 67(15): 1553-1555.

LIU B, MA J X, LI P F, et al., 2025. First boron isotopes in the southern Jilin TTG series uncover a Neoarchean oceanic arc in the eastern North China Craton[J]. Gondwana Research, 139: 243-259.

LIU D Y, NUTMAN A P, COMPSTON W, et al., 1992. Remnants of ≥3800 Ma crust in the Chinese part of the Sino-Korean craton[J]. Geology, 20(4): 339-342.

LIU G, LU J S, ZHAI M G, et al., 2022. Clockwise P–T–t paths of late Neoarchean high-pressure pelitic granulites from the Qingyuan terrane, eastern North China Craton[J]. Precambrian Research, 381: 106874.

LIU J H, LIU F L, DING Z J, et al., 2024a. Mesoarchean–Neoarchean coupled crust–mantle differentiation followed by gravity-driven lithospheric delamination and subduction initiation in the North China Craton[J]. Precambrian Research, 404: 107349.

LIU S, FENG C X, SANTOSH M, et al., 2019. Origin and geodynamics of Neoarchean mafic dikes in Western Shandong, Northeastern North China Craton: geochronological, geochemical, and Nd-Hf isotopic evidence[J]. The Journal of Geology, 127(1): 61-79.

LIU S W, BAO H, GAO L, et al., 2021. Late Neoarchean metavolcanics and geodynamics regime in central and eastern North China Craton[J]. Acta Petrologica Sinica, 37(1): 113-128. (in Chinese with English abstract)

LIU T, WEI C J, JOHNSON T E, 2024b. Archean UHT metamorphism with counterclockwise P–T path: insights from pelitic granulites from East Hebei, North China Craton[J]. Gondwana Research, 133: 108-128.

LU C S, QIAN J H, YIN C Q, et al., 2023. Characterising early Precambrian collisional orogens: a metamorphic perspective from the Lüliang Com-

plex and the Trans-North China Orogen[J]. Earth-Science Reviews, 245: 104566.

LU S N, CHEN Z H, XIANG Z Q, 2008. Geochronological framework of ancient intrusions in Taishan Geopark[M]. Beijing: Geological Publishing House: 1-90. (in Chinese)

MANIAR P D, PICCOLI P M, 1989. Tectonic discrimination of granitoids[J]. GSA Bulletin, 101(5): 635-643.

MARTIN H, SMITHIES R H, RAPP R, et al., 2005. An overview of adakite, tonalite–trondhjemite–granodiorite (TTG), and sanukitoid: relationships and some implications for crustal evolution[J]. Lithos, 79(1-2): 1-24.

MARTIN H, MOYEN J F, RAPP R, 2009. The sanukitoid series: magmatism at the Archaean–Proterozoic transition[J]. Earth and Environmental Science Transactions of the Royal Society of Edinburgh, 100(1-2): 15-33.

MCDONOUGH W F, 2003. Compositional model for the earth's core[J]. Treatise on Geochemistry, 2: 547-568.

MOYEN J F, MARTIN H, JAYANANDA M, et al., 2003. Late Archaean granites: a typology based on the Dharwar Craton (India)[J]. Precambrian Research, 127(1-3): 103-123.

MU M S, YANG D B, YANG H T, et al., 2022. Petrogenesis and tectonic implications of the Paleoproterozoic Gaoliduntai plagiogranites in the Jiao–Liao–Ji Belt, North China Craton[J]. Precambrian Research, 368: 106465.

O'CONNOR J T, 1965. A classification for quartz-rich igneous rocks based on feldspar ratios[J]. US Geological Survey, Professional Papers, 525B: B79-B84.

OLIVEIRA E P, SOUZA Z S, MCNAUGHTON N J, et al., 2011. The Rio Capim volcanic-plutonic-sedimentary belt, São Francisco Craton, Brazil: geological, geochemical and isotopic evidence for oceanic arc accretion during Palaeoproterozoic continental collision[J]. Gondwana Research, 19(3): 735-750.

OUYANG D J, JIAO S J, COLLINS W J, et al. , 2024. Evolution of A-type granites during the Late Paleoproterozoic orogenic cycle of North China craton: implications for post-collisional magmatism[J]. Lithos, 474-475: 107584.

PALIN R M, SANTOSH M, CAO W T, et al., 2020. Secular change and the onset of plate tectonics on Earth[J]. Earth-Science Reviews, 207: 103172.

PEARCE J A, 1983. Role of the sub-continental lithosphere in magma genesis at active continental margins[M]//HAWKESWORTH C J, NORRY M J. Continental basalts and mantle xenoliths. Nantwich: Shiva Publishing: 158-185.

PENG T P, FAN W M, PENG B X, 2012. Geochronology and geochemistry of late Archean adakitic plutons from the Taishan granite-greenstone Terrain: implications for tectonic evolution of the eastern North China Craton[J]. Precambrian Research, 208-211: 53-71.

PENG T P, WILDE S A, FAN W M, et al., 2013. Neoarchean siliceous high-Mg basalt (SHMB) from the Taishan granite-greenstone terrane, Eastern North China Craton: petrogenesis and tectonic implications[J]. Precambrian Research, 228: 233-249.

PERCHUK A L, SAFONOV O G, SMIT C A, et al., 2018. Precambrian ultrahot orogenic factory: making and reworking of continental crust[J]. Tectonophysics, 746: 572-586.

POLAT A, HERZBERG C, MUNKER C, et al., 2006. Geochemical and petrological evidence for a suprasubduction zone origin of Neoarchean (ca. 2.5 Ga) peridotites, central orogenic belt, North China craton[J]. GSA Bulletin, 118(7-8): 771-784.

REN P, XIE H Q, WANG S J, et al., 2016. A ca. 2.60 Ga tectono-thermal event in Western Shandong Province, North China Craton from zircon U–Pb–O isotopic evidence: plume or convergent plate boundary process[J]. Precambrian Research, 281: 236-252.

ROJAS-AGRAMONTE Y, KRÖNER A, DEMOUX A, et al., 2011. Detrital and xenocrystic zircon ages from Neoproterozoic to Palaeozoic arc terranes of Mongolia: significance for the origin of crustal fragments in the Central Asian Orogenic Belt[J]. Gondwana Research, 19(3): 751-763.

SAFONOVA I, 2017. Juvenile versus recycled crust in the Central Asian Orogenic Belt: implications from ocean plate stratigraphy, blueschist belts and intra-oceanic arcs[J]. Gondwana Research, 47: 6-27.

SAFONOVA I Y, SANTOSH M, 2014. Accretionary complexes in the Asia-Pacific region: tracing archives of ocean plate stratigraphy and tracking mantle plumes[J]. Gondwana Research, 25(1): 126-158.

SANTOSH M, MARUYAMA S, KOMIYA T, et al., 2010. Orogens in the evolving Earth: from surface continents to 'lost continents' at the core-mantle boundary[J]. Geological Society, London, Special Publications, 338(1): 77-116.

SANTOSH M, LIU D Y, SHI Y R, et al., 2013. Paleoproterozoic accretionary orogenesis in the North China Craton: a SHRIMP zircon study[J]. Precambrian Research, 227: 29-54.

SANTOSH M, TENG X M, HE X F, et al., 2016. Discovery of Neoarchean suprasubduction zone ophiolite suite from Yishui Complex in the North China Craton[J]. Gondwana Research, 38: 1-27.

SANTOSH M, GAO P, YU B, et al., 2020. Neoarchean suprasubduction zone ophiolite discovered from the Miyun Complex: implications for Archean–Paleoproterozoic Wilson cycle in the North China Craton[J]. Precambrian Research, 342: 105710.

Shandong Institute of Geological Survey, 2021. Regional geology of China, Shandong Province[M]. Beijing: Geological Publishing House. (in Chinese)

SHI K X, WANG C M, SANTOSH M, et al., 2019. New insights into Neoarchean–Paleoproterozoic crustal evolution in the North China Craton: evidence from zircon U-Pb geochronology, Lu–Hf isotopes and geochemistry of TTGs and greenstones from the Luxi Terrane[J]. Precambrian Research, 327: 232-254.

SHU L S, YAO J L, WANG B, et al., 2021. Neoproterozoic plate tectonic process and Phanerozoic geodynamic evolution of the South China Block[J]. Earth-Science Reviews, 216: 103596.

SONG M C, JIAO X M, SONG Y X, et al., 2011. Geochemical characteristics and sedimentary environment of Precambrian Jining Group in Western Shandong Province[J]. Geotectonica et Metallogenia, 35(4): 543-551. (in Chinese with English abstract)

STERN R J, TSUJIMORI T, HARLOW G, et al., 2013. Plate tectonic gemstones[J]. Geology, 41(7): 723-726.

SUN G Z, LIU S W, GAO L, et al., 2019a. Neoarchean sanukitoids and associated rocks from the Tengzhou-Pingyi intrusive complex, North China Craton: insights into petrogenesis and crust-mantle interactions[J]. Gondwana Research, 68: 50-68.

SUN G Z, LIU S W, SANTOSH M, et al., 2019b. Thickness and geothermal gradient of Neoarchean continental crust: inference from the southeastern North China Craton[J]. Gondwana Research, 73: 16-31.

SUN G Z, LIU S W, GAO L, et al., 2020. Origin of late Neoarchean granitoid diversity in the Western Shandong province, North China Craton[J]. Precambrian Research, 339: 105620.

SUN G Z, LIU S W, CAWOOD P A, et al., 2021. Thermal state and evolving geodynamic regimes of the Meso-to Neoarchean North China Craton[J]. Nature Communications, 12(1): 3888.

SUN G Z, LIU S W, WANG L T, et al., 2025. Late Neoarchean sanukitoids in the North China Craton: a geodynamic perspective[J]. Geosystems and Geoenvironment, 4(4): 100426.

TIAN Z H, NUTMAN A P, 2022. Structural restoration of an Eo-Mesoarchean (3.8-2.9 Ga) terrane, Eastern China, dissected by the Tanlu fault zone[J]. Journal of Structural Geology, 161: 104629.

WAN Y S, LIU D Y, WANG S J, et al., 2010. Juvenile magmatism and crustal recycling at the end of the Neoarchean in Western Shandong Province, North China Craton: evidence from SHRIMP zircon dating[J]. American Journal of Science, 310(10): 1503-1552.

WAN Y S, LIU D Y, WANG S J, et al., 2011. 2.7 Ga juvenile crust formation in the North China Craton (Taishan-Xintai area, western Shandong Province): further evidence of an understated event from U–Pb dating and Hf isotopic composition of zircon[J]. Precambrian Research, 186(1-4): 169-180.

WAN Y S, WANG S J, LIU D Y, et al., 2012a. Redefinition of depositional ages of Neoarchean supracrustal rocks in western Shandong Province, China: SHRIMP U-Pb zircon dating[J]. Gondwana Research, 21(4): 768-784.

WAN Y S, DONG C Y, LIU D Y, et al. , 2012b. Zircon ages and geochemistry of late Neoarchean syenogranites in the North China Craton: a review[J]. Precambrian Research, 222-223: 265-289.

WAN Y S, XIE S W, YANG C H, et al., 2014a. Early Neoarchean (～2.7Ga) tectono–thermal events in the North China Craton: a synthesis[J]. Precambrian Research, 247: 45-63.

WAN Y S, DONG C Y, WANG S J, et al., 2014b. Middle Neoarchean magmatism in western Shandong, North China Craton: SHRIMP zircon dating and LA-ICP-MS Hf isotope analysis[J]. Precambrian Research, 255: 865-884.

WAN Y S, MA M Z, DONG C Y, et al., 2015. Widespread late Neoarchean reworking of Meso-to Paleoarchean continental crust in the Anshan-Benxi area, North China Craton, as documented by U-Pb-Nd-Hf-O isotopes[J]. American Journal of Science, 315(7): 620-670.

WAN Y S, GUO R P, TIAN J X, et al. , 2019. Discovery of Mesoarchean-early Neoarchean TTG Rocks in Laizhou Area in Eastern Shandong of North China Craton: SHRIMP U-Pb zircon dating[J]. Shandong Land and Resources, 35(4): 1-16, 37. (in Chinese with English abstract)

WAN Y S, DONG C Y, XIE H Q, et al., 2023. Hadean to early Mesoarchean rocks and zircons in the North China Craton: a review[J]. Earth-Science Reviews, 243: 104489

WANG A D, LIU Y C, 2012. Neoarchean (2.5-2.8 Ga) crustal growth of the North China Craton revealed by zircon Hf isotope: a synthesis[J]. Geoscience Frontiers, 3(2): 147-173.

WANG D M, HU J M, ZHAO Y F, et al., 2024a. Kinematics and geochronology of the ductile shear zones in the western Shandong granite-greenstone belt: implications for the Neoarchean plate tectonics of the North China Craton[J]. Precambrian Research, 411: 107509.

WANG J P, KUSKY T, POLAT A, et al., 2013a. A late Archean tectonic mélange in the Central orogenic belt, North China Craton[J]. Tectonophysics, 608: 929-946.

WANG K, LIU S W, WANG M J, et al., 2017a. Geochemistry and zircon U-Pb-Hf isotopes of the late Neoarchean granodiorite-monzogranite-quartz syenite intrusions in the Northern Liaoning Block, North China Craton: petrogenesis and implications for geodynamic processes[J]. Precambrian Research, 295: 151-171.

WANG W, WANG S J, DONG C Y, et al., 2010. SHRIMP U-Pb dating of zircons from Neoarchean crustal derived granites in the Lushan area, Shandong, China[J]. Geological Bulletin of China, 29(7): 993-1000. (in Chinese with English abstract)

WANG W, YANG E X, ZHAI M G, et al., 2013b. Geochemistry of～ 2.7 Ga basalts from Taishan area: constraints on the evolution of early Neoarchean granite-greenstone belt in western Shandong Province, China[J]. Precambrian Research, 224: 94-109.

WANG W, ZHAI M G, WANG S J, et al., 2013c. Crustal reworking in the North China Craton at ～ 2.5 Ga: evidence from zircon U–Pb age, Hf isotope and whole rock geochemistry of the felsic volcano-sedimentary rocks from the western Shandong Province[J]. Geological Journal, 48(5): 406-428.

WANG W, ZHAI M G, TAO Y B, et al., 2014. Late Neoarchean crustal evolution of the eastern North China Craton: a study on the provenance and metamorphism of paragneiss from the Western Shandong Province[J]. Precambrian Research, 255: 583-602.

WANG W, LIU S W, SANTOSH M, et al., 2015. Neoarchean intra-oceanic arc system in the Western Liaoning Province: implications for Early Precambrian crustal evolution in the Eastern Block of the North China Craton[J]. Earth-Science Reviews, 150: 329-364.

WANG W, ZHAI M G, SANTOSH M, 2016. The genesis of Archean supracrustal rocks in the western Shandong Province of North China Craton: constraints on regional crustal evolution[J]. Science China Earth Sciences, 59(8): 1583-1596.

WANG W, ZHAI M G, WANG S J, et al., 2016a. Neoarchean crustal evolution in western Shandong Province of the North China Craton: the role of 2.7-2.6 Ga magmatism[J]. Precambrian Research, 285: 170-185.

WANG W, LIU S W, CAWOOD P A, et al., 2016b. Late Neoarchean subduction-related crustal growth in the Northern Liaoning region of the North China Craton: evidence from～ 2.55 to 2.50 Ga granitoid gneisses[J]. Precambrian Research, 281: 200-223.

WANG W, ZHANG X, WANG S J, et al., 2017b. Geochronology and geochemistry of Neoarchean granitoids from the western Shandong Province, North China Craton, implications for crustal evolution and cratonization[J]. Precambrian Research, 303: 749-763.

WANG W, CAWOOD P A, LIU S W, et al., 2017c. Cyclic formation and stabilization of Archean lithosphere by accretionary orogenesis: constraints from TTG and potassic granitoids, North China Craton[J]. Tectonics, 36(9): 1724-1742.

WANG W, LIU S W, CAWOOD P A, et al., 2024b. Early Neoarchean alternation of plate subduction and deep mantle upwelling[J]. Precambrian Research, 402: 107303.

WANG X, ZHU W B, ZHENG Y F, 2022. Geochemical constraints on the nature of Late Archean basaltic-andesitic magmatism in the North China Craton[J]. Earth-Science Reviews, 230: 104065.

WANG X, GE R F, ZHENG Y F, et al., 2024c. Successful subduction of oceanic plate after failed attempts in the Late Archean: petrological and geochemical constraints[J]. Earth and Planetary Science Letters, 644: 118944.

WANG X S, ZHUANG Y X, XU H F, et al., 1999. The implication of terminal Archean ductile shearing in continental crustal evolution of the Taishan Mountain region[J]. Regional Geology of China, 18(2): 168-174. (in Chinese with English abstract)

WANG Y J, ZHAO G C, FAN W M, et al., 2007. LA-ICP-MS U–Pb zircon geochronology and geochemistry of Paleoproterozoic mafic dykes from western Shandong Province: implications for back-arc basin magmatism in the Eastern Block, North China Craton[J]. Precambrian Research, 154(1-2): 107-124.

WANG Y J, ZHANG Y Z, ZHAO G C, et al., 2009. Zircon U-Pb geochronological and geochemical constraints on the petrogenesis of the Taishan sanukitoids (Shandong): implications for Neoarchean subduction in the Eastern Block, North China Craton[J]. Precambrian Research, 174(3-4): 273-286.

WANG Y Q, DONG C Y, WILDE S A, et al., 2025. The Neoarchean granitoids in the Yanlingguan area, western Shandong, North China Craton record the transition from TTG to K-rich granitoids[J]. Precambrian Research, 417: 107633.

WANG Z H, 2009. Tectonic evolution of the Hengshan-Wutai-Fuping complexes and its implication for the Trans-North China Orogen[J]. Precambrian Research, 170(1-2): 73-87.

WEI C M, YAO Y Z, FU J F, et al., 2025. Diverse provenances and tectonic setting of late Neoarchean metasedimentary rocks from the Anshan-Benxi greenstone belt, North China Craton: constraints from whole-rock geochemistry and zircon U–Pb–Lu–Hf isotopes[J]. Journal of Asian Earth Sciences, 279: 106443.

WU M L, LIN S F, WAN Y S, et al., 2021. Episodic Archean crustal accretion in the North China Craton: insights from integrated zircon U-Pb-Hf-O isotopes of the Southern Jilin Complex, northeast China[J]. Precambrian Research, 358: 106150.

WU M L, ZHAO G C, SUN M, et al. , 2013. Zircon U-Pb geochronology and Hf isotopes of major lithologies from the Yishui Terrane: implications for the crustal evolution of the Eastern Block, North China Craton[J]. Lithos, 170-171: 164-178.

XIAO W J, SANTOSH M, 2014. The western Central Asian Orogenic Belt: a window to accretionary orogenesis and continental growth[J]. Gondwana Research, 25(4): 1429-1444.

XIAO W J, LI J L, SONG D F, et al., 2019. Structural analyses and spatio-temporal constraints of Accretionary Orogens[J]. Earth Science, 44(5): 1661-1687. (in Chinese with English abstract)

YAKYMCHUK C, ZHAO W R, WAN Y S, et al. , 2019. Fluid-present anatexis of Neoarchean tonalite and amphibolite in the Western Shandong Province[J]. Lithos, 326-327: 110-124.

YANG F, SANTOSH M, KIM S W, et al., 2021. Late Neoarchean to Paleoproterozoic arc magmatism in the Shandong Peninsula, North China Craton and its tectonic implications[J]. Precambrian Research, 358: 106188.

YANG J, WU F, WILDE S, et al., 2008. Petrogenesis and geodynamics of late Archean magmatism in Eastern Hebei, eastern North China Craton: geochronological, geochemical and Nd–Hf isotopic evidence[J]. Precambrian Research, 167(1-2): 125-149.

YANG L H, HOU G T, LIU S W, et al., 2019. 2.09 Ga mafic dykes from Western Shandong, Eastern block of North China Craton, and their tectonic implications[J]. Precambrian Research, 325: 39-54.

YANG L H, HOU G T, GAO L, et al., 2020. Neoarchaean subduction tectonics in Western Shandong Province, China: evidence from geochemistry and zircon U–Pb–Hf isotopes of metabasalts[J]. Geological Journal, 55(5): 3575-3600.

YANG Q Y, SANTOSH M, COLLINS A S, et al., 2016a. Microblock amalgamation in the North China Craton: evidence from Neoarchaean magmatic suite in the western margin of the Jiaoliao Block[J]. Gondwana Research, 31: 96-123.

YANG Q Y, SANTOSH M, TSUNOGAE T, 2016b. High-grade metamorphism during Archean–Paleoproterozoic transition associated with microblock amalgamation in the North China Craton: mineral phase equilibria and zircon geochronology[J]. Lithos, 263: 101-121.

YANG Q Y, SANTOSH M, 2017. The building of an Archean microcontinent: evidence from the North China Craton[J]. Gondwana Research, 50: 3-37.

YU Y, LI D P, CHEN Y L, et al. , 2019. Late Neoarchean slab rollback in the Jiaoliao microblock, North China craton: constraints from zircon U-Pb geochronology and geochemistry of the Yishui complex, Western Shandong province[J]. Lithos, 342-343: 315-332.

YU Y, LI D P, CHEN Y L, et al., 2021. Mantle cooling and cratonization of Archean lithosphere by continuous plate subduction: constraints from TTGs, sanukitoids, and high-K granites, eastern North China Craton[J]. Precambrian Research, 353: 106042.

YU Y, LI D P, CHEN Y L, et al., 2022. Mesoarchean trondhjemitic continental nucleus and pre-plate tectonic crustal-mantle interactions of the Western Shandong Complex, North China Craton[J]. Precambrian Research, 369: 106517.

ZHAI M G, GUO J H, LIU W J, 2005. Neoarchean to Paleoproterozoic continental evolution and tectonic history of the North China Craton: a review[J]. Journal of Asian Earth Sciences, 24(5): 547-561.

ZHAI M G, SANTOSH M, 2011. The early Precambrian odyssey of the North China Craton: a synoptic overview[J]. Gondwana Research, 20(1): 6-25.

ZHAI M G, 2014. Multi-stage crustal growth and cratonization of the North China Craton[J]. Geoscience Frontiers, 5(4): 457-469.

ZHAI M G, ZHAO L, ZHU X Y, et al., 2020. Review and overview for the frontier hotspot: early continents and start of plate tectonics[J]. Acta Petrologica Sinica, 36(8): 2249-2275. (in Chinese with English abstract)

ZHANG H, HOU G T, ZHANG B, et al., 2022. Kinematics, temperature and geochronology of the Qingyi ductile shear zone: tectonic implications for

late Neoarchean microblock amalgamation in the Western Shandong Province, North China craton[J]. Journal of Structural Geology, 161: 104645.

ZHANG H, HOU G T, TIAN W, 2023. Baddeleyite dating of a 2.34 Ga mafic dyke in the Western Shandong Province, North China Craton, and its tectonic implications[J]. Lithos, 438-439: 107013.

ZHANG H T, LI Y L, ZHENG J P, et al., 2024. The Archean crust-mantle interaction in the Jiaoliao microblock, North China Craton: constraints on the Neoarchean subduction regime[J]. Earth-Science Reviews, 255: 104827.

ZHANG S H, ZHOU X Q, 1999. Microstructure study and petrofabric analyses of the ductile shear zones in western Shandong[J]. Contributions to Geology and Mineral Resources Research, 14(1): 39-47. (in Chinese with English abstract)

ZHANG S H, ZHANG J, ZHAO C, et al., 2025. Deformational characteristics of the Qixingtai ductile shear zone, western Shandong: implications for the Neoarchean tectonic evolution of the eastern North China Craton[J]. Acta Petrologica Sinica, 41(1): 237-259. (in Chinese with English abstract)

ZHANG Y, XIE W, LI D P, et al., 2025b. Depositional age and source material of banded iron formations in the Western Shandong Province, North China Craton: constraints from geochemistry, zircon U–Pb geochronology and Sm–Nd isotope composition[J]. Journal of Geochemical Exploration, 271: 107691.

ZHANG Z Q, YANG E X, LIU R P, et al., 2012. Geological characteristics of Longting Rubby Deposit in Xintai City of Shandong Province[J]. Shandong Land and Resources, 28(1): 1-4. (in Chinese with English abstract)

ZHAO G C, KRÖNER A, WILDE S A, et al., 2007. Lithotectonic elements and geological events in the Hengshan–Wutai–Fuping belt: a synthesis and implications for the evolution of the Trans-North China Orogen[J]. Geological Magazine, 144(5): 753-775.

ZHAO G C, ZHAI M G, 2013. Lithotectonic elements of Precambrian basement in the North China Craton: review and tectonic implications[J]. Gondwana Research, 23(4): 1207-1240.

ZHENG Y F, ZHAO G C, 2020. Two styles of plate tectonics in Earth's history[J]. Science Bulletin, 65(4): 329-334.

ZHONG Y T, KUSKY T, WANG L, et al., 2021. Alpine-style nappes thrust over ancient North China continental margin demonstrate large Archean horizontal plate motions[J]. Nature Communications, 12(1): 6172.

ZUO R, LONG X P, WU B, et al., 2025. Petrogenesis of the > 2.90 Ga komatiite in the Sujiagou region of the North China Craton: implications for Archean mantle source and geodynamic setting[J]. Precambrian Research, 417: 107632.

附中文参考文献

曹国权，1996. 鲁西早前寒武纪地质[M]. 北京：地质出版社：1-210.

杜利林，庄育勋，杨崇辉，等，2003. 山东新泰孟家屯岩组锆石特征及其年代学意义[J]. 地质学报，77(3)：359-366.

杜利林，庄育勋，杨崇辉，等，2005. 鲁西孟家屯一种细粒斜长角闪岩的锆石 SHRIMP 年代学[J]. 地球学报，26(5)：429-434.

刘树文，包涵，高磊，等，2021. 华北克拉通中东部新太古代晚期变质火山岩及动力学体制[J]. 岩石学报，37(1)：113-128.

陆松年，陈志宏，相振群，2008. 泰山世界地质公园古老侵入岩系年代格架[M]. 北京：地质出版社：1-90.

山东省地质调查院，2021. 中国区域地质志：山东志[M]. 北京：地质出版社.

宋明春，焦秀美，宋英昕，等，2011. 鲁西隐伏含铁岩系：前寒武纪济宁岩群地球化学特征及沉积环境[J]. 大地构造与成矿学，35(4)：543-551.

万渝生，郭瑞朋，田京祥，等，2019. 华北克拉通胶东莱州地区中太古代-新太古代早期 TTG 岩石的发现：锆石 SHRIMP U-Pb 定年[J]. 山东国土资源，35(4)：1-16, 37.

王伟，王世进，董春艳，等，2010. 山东鲁山地区新太古代壳源花岗岩锆石 SHRIMP U-Pb 定年[J]. 地质通报，29(7)：993-1000.

王伟，翟明国，SANTOSH M, 2016. 鲁西太古宙表壳岩的成因及其对地壳演化的制约[J]. 中国科学：地球科学，46(7)：949-962.

王新社，庄育勋，徐惠芬，等，1999. 泰山地区太古宙末韧性剪切作用在陆壳演化中的意义[J]. 中国区域地质，18(2)：168-174.

肖文交，李继亮，宋东方，等，2019. 增生型造山带结构解析与时空制约[J]. 地球科学，44(5)：1661-1687.

翟明国，赵磊，祝禧艳，等，2020. 早期大陆与板块构造启动：前沿热点介绍与展望[J]. 岩石学报，36(8)：2249-2275.

张书慧，张健，赵辰，等，2025. 鲁西七星台地区韧性剪切带变形特征及样式：对华北克拉通东部新太古代演化的构造约束[J]. 岩石学报，41(1)：237-259.

张拴宏，周显强，1999. 鲁西地区韧性剪切带显微构造研究及岩组分析[J]. 地质找矿论丛，14(1)：39-47.

张增奇，杨恩秀，刘鹏瑞，等，2012. 鲁西地区“泰山红宝石”的发现及其地质特征[J]. 山东国土资源，28(1)：1-4.